The Time-dependent Response of Concrete Bond to Steel Under High Sustained Loads

---

A Thesis presented to

the Faculty of the Graduate School at

the University of Missouri – Columbia

In Partial Fulfillment of the Requirements for the Degree

Master of Science in

Civil Engineering

---

by

PHILIP SWOBODA

Dr. Sarah Orton, Thesis Supervisor

December 2020

The undersigned, appointed by the dean of the Graduate School, have examined the thesis entitled:

The Time-dependent Response of Concrete Bond to Steel Under High Sustained Loads

Presented by Philip Swoboda,

a candidate for the degree of Master of Science in Civil Engineering,

and hereby certify that, in their opinion, it is worthy of acceptance.

_____

Professor Sarah Orton

_____

Professor Hani Salim

_____

Professor Sanjeev Khanna

ACKNOWLEDGMENTS

I would like to thank my faculty advisor and thesis supervisor Dr. Sarah Orton for helping me through the process of conducting research and writing this thesis. She provided great direction and encouragement throughout the entire process.

I would also like to thank Mohammed Shubaili, David Treece, and Ali Elawadi for assisting me in construction and testing of the test setup and the specimens used in this research project.

Thank you to the other members of my thesis committee Dr. Hani Salim and Dr. Sanjeev Khanna for taking the time to provide me with thorough feedback.

Thank you to Mike Carraher for providing valuable help in troubleshooting electrical problems that arose throughout testing. Also thank you to Dr. Aaron Saucier for general advice and assistance when working at the lab.

Table of Contents

LIST OF FIGURES

ABSTRACT

Design errors, poor construction practices, material deterioration, and other issues can lead to reinforced concrete members being subjected to levels of sustained stresses higher than their expected service loads. These high levels of sustained stress have led to catastrophic RC building collapses around the world. Loading a member greater than $0.75f_c'$ is referred to as high sustained loading and is in the range that could potentially lead to the progressive collapse of a structure. Unfortunately, the behavior of concrete members under this loading condition is not well understood. By gaining understanding of member's behavior when loaded under high sustained stresses, future engineers can better identify elements nearing failure.

Preliminary tests performed on simple RC beams tested in flexure showed the beams' tendency to increase in deflection with time – more than the expected creep deflection. This extra deflection occurring at high sustained loading may be accounted for by slippage between the reinforcing bar and the concrete. In order to isolate and study this bond slippage under high sustained loads, beam-end bond tests were loaded to 85-90% of their short-term capacity and observed for several weeks. The tests show that continued slipping is occurring under high sustained loads. The first sustained load test experienced 22% of its overall slip when under sustained load. The first sustained test also withheld a bond load of 12% more than the control specimens. The three sustained specimens experienced an increase in free end slip from 0.001" to 0.00254" under constant load which is 90% to 230% of the slip at failure in the control specimen. This slip under high levels of sustained load may contribute to the additional deflection under sustained load in reinforced concrete members.

Chapter I Introduction

The bond between steel reinforcement and concrete is required to transfer tensile stresses. This transfer of stress is a key component in the behavior of a reinforced concrete member. While the over mechanism of bond is well understood, the time-dependent bond behavior under high levels of stress is not. This thesis gives an in-depth look at these time-dependent characteristics in order to better explain the behavior of reinforced concrete at high levels of stress.

1.1 Brief history of time-dependent concrete properties

Observations that concrete properties vary and develop with time are well documented since concrete's discovery. John Smeaton, considered to be the "Father of Modern Concrete", wrote about the tendency of concrete to change with time as early as 1791. Smeaton's observations mainly focused on the increase in strength and stiffness with time, due to the continued process of cement hydration. The creep effect in concrete wasn't discovered until around 1910 when French engineer Eugene Fryssinet observed large deflections of the three span Le Veurdre concrete bridge. These large deflections, which were increasing with time, prompted Fryssinet to discover concrete creep.

Fifty years later, Hubert Rüsch proposed a General Flexural Theory for structural concrete members. This theory introduced the concept of structural member failure due to high sustained loading. Rüsch had discovered that the amount of load placed on a concrete member has a large effect on the creep that the member experiences; in fact, if the load is large enough, a member may fail years after the initial loading. Rüsch then

introduced the concept of a “sustained load strength” in concrete. The sustained load strength is the amount of load that can be placed on a concrete member without risk of failure due to creep over time. Rüsch proposed that the sustained load strength of concrete is 75% of the ultimate strength of the member.

The discovery of a possibility of failure when under high sustained loading (loading at or above 75% of the strength of the member) has influenced concrete design practices. Most design codes, such as the American Concrete Institute (ACI) account for this by reducing the overall capacity of the member by 85%. In theory, this, along with other factors of safety, lowers the probability of failure of a RC structure enough that it is deemed safe.

1.2 Consequences of high sustained loading

Well-designed reinforced concrete (RC) structures perform well under normal service loading conditions. It is not until a member experiences overloading (more load than the recommended design load) that problems arise. This overloading can be caused by construction errors, material degradation, or design errors. Whatever the cause, this overloading places RC members under high levels of sustained stress which may eventually lead to failure of the member. Overloaded member failure can lead to progressive collapse of buildings.

An example of failure under sustained load took place on February 2, 2004, in Konya, Turkey. A 9-story apartment building known as the Zumrut collapsed 4 years after construction was finished (Figure 1). The collapse of this 9-story reinforced concrete building left 92 people dead. Mistakes in design and careless construction resulted in

several crucial members being overloaded. The high sustained stresses experienced by these members resulted in large nonlinear creep and eventual failure of the structure [Tasevski,2019]. The Zumrut tragedy is just one example of the devastating result that delayed failure in RC members can cause.

Figure 1: The Zumrut Apartment Building in Koyta, Turkey: (a) Structural Layout, (b) nonlinear creep damage of basement columns, (c) Collapse of the building [Tasevski,2019].

Another tragic case of an RC building demonstrating time-dependent collapse occurred in Seoul, South Korea. In 1995, the Sampoog Department Store collapsed during peak shopping hours, killing over 500 people. Management had closed parts of the store as irregular cracks in the concrete had been noticed on several stores months before collapse took place. Not recognizing the potential danger, the cracks were ignored. Investigations conducted after the collapse revealed that the building was loaded past the design loads and that the columns were constructed with nearly half of the designed capacity. This almost certainly placed members of this structure in the range of high-sustained loading.

While the most tragic examples have occurred elsewhere, the United States is not immune to this type of building collapse. In fact, between the years of 1989-2000, 172

RC buildings in the US alone have experienced structural failures [Wardhana,2003]. Most of these failures, like the Wilson Hospital parking garage collapse in 2015 in New York, happened under sustained gravity loads. Better understanding of concrete behavior under high sustained loads will be helpful in recognizing and preventing collapses from occurring in the future.

1.3 Overall research project overview

This thesis is a subset of a larger project trying to understand the impact that sustained gravity loads have on the progressive collapse of large-scale reinforced concrete buildings. This project, led by Dr. Sarah Orton at the University of Missouri and Dr. Ying Tian at the University of Nevada Las Vegas, is attempting to answer two key scientific questions:

- What are the time-dependent strength and stiffness characteristics of reinforced concrete members under sustained high stresses?
- What is the system level response of a reinforced concrete building near collapse when a critical component has experienced failure?

The current knowledge of reinforced concrete's time-dependent response to high levels of loading is not sufficient in answering these two questions. By studying the behavior of concrete under high sustained stresses, a better understanding can be gained of fundamental characteristics of concrete which are needed to recognize and predict building collapse evolution (Figure 2).

Figure 2: Justification of this research project.

While completing the overall research project, it was found that the behavior of reinforcement to concrete bond has significant impact on the behavior of a RC structure under high sustained gravity loads. Therefore, the objectives of this thesis are:

- To investigate the behavior of the bond between concrete and reinforcing bars under high sustained loads.
- To evaluate the interaction between the deformed reinforcing bars and the surrounding concrete in order to better explain behavior of RC members subjected to high sustained loading.

Chapter II Literature Review

2.1 Introduction to time-dependent deformations

Plain concrete experiences three types of time-dependent deformations: shrinkage, creep, and thermal expansion. These three can cause stresses, cracking, or deformation that affect the long-term behavior of reinforced concrete structures [Wight,2009]. All of these impacts the behavior of concrete structures and must be examined when studying time-dependent characteristics of concrete.

2.2 Shrinkage

Hygro-thermal strain, also known as shrinkage, relates to the interaction of water and cement paste in concrete which causes strain to occur over time. Exposing concrete to a dry atmosphere allows free water, which previously is absorbed inside the hardened Portland cement, to diffuse out of the cement gel micropores. The microstructure of hardened Portland cement contains a large amount of free water. When a cement capillary loses some of its water, the remaining water forms a curved meniscus along the walls of the pore which produces surface tension that pulls the walls of the pore inward. This creates internal negative pressure which is enough to cause an overall decrease in volume of the specimen [Bazant, 1975]. This, along with the actual loss of free pore water evaporating out of the concrete, is the reason plain concrete experiences drying shrinkage. [Bazant, 1975].

All concrete experiences shrinkage unless the specimen is in an environment of 100% humidity. Concrete in a dry atmosphere (Figure 3) experiences the majority of shrinkage early on; the drying shrinkage rate decreases towards a finite bound with the age of the concrete [Bazant, 1975].

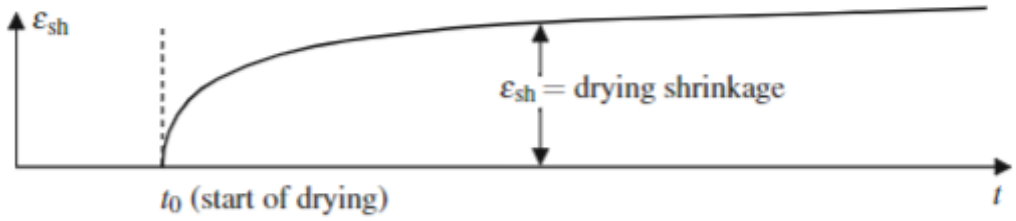

Figure 3: Strain vs. Time graph of drying shrinkage [Bazant, 2018].

This paper will not go into detail discussing shrinkage strain. The specimens tested in this project are left to age for several months before testing. This is old enough that most of the drying shrinkage occurs prior to testing. However, testing conditions prevented a constant humidity environment. Instead the humidity during the testing was monitored. Although, the shrinkage that occurred during testing is likely negligible compared to the mechanical and creep strain experienced by the specimen some effects of shrinkage may have occurred.

2.3 Thermal Expansion

Thermal expansion is a material's tendency to increase in volume as it increases in temperature. For concrete, the amount of expansion is affected by the composition of the concrete, the age of the concrete, and the moisture content [Wight,2009]. There are different coefficients of thermal expansion for different mix designs. A coefficient of

thermal expansion is used to predict the expected strain experienced per degree of temperature rise; these coefficients are used when designing for thermal expansion. Steel has a separate coefficient of thermal expansion and thus will expand or contract at a different rate than the concrete. Steel is also a much better conductor than concrete, this property makes steel more susceptible to temperature changes. This is one example of a discontinuity between concrete and steel in RC. Again, the testing conditions prevented a constant temperature environment. The temperature was measured during testing and may have some minor effects in the response of the specimen.

2.4 Creep

The third type of time-dependent strain happens when stress is applied to a concrete specimen causing mechanical strain to occur. This type of strain is referred to as creep. Creep is the tendency of a material to have an increase in strain even when stress is held constant. Figure 4.a shows a constant load being applied while Figure 4.b shows the strain response that concrete cylinder has to the loading. Applying the stress causes an instantaneous strain known as elastic strain. This elastic strain begins by following Hooke's Law in which the strain is directly proportional to the applied stress; this proportionality is the linear portion of the strain vs. time graph (Figure 4.b). The specimen then begins to experience creep strain directly after the instantaneous strain occurs. Creep strain increases at a gradually decreasing rate that continues for the duration of the loading [Bazant, 2018]. Once the specimen is unloaded, it experiences an instantaneous elastic recovery; this is followed by a nonlinear creep recovery that approaches a finite bound.

a)

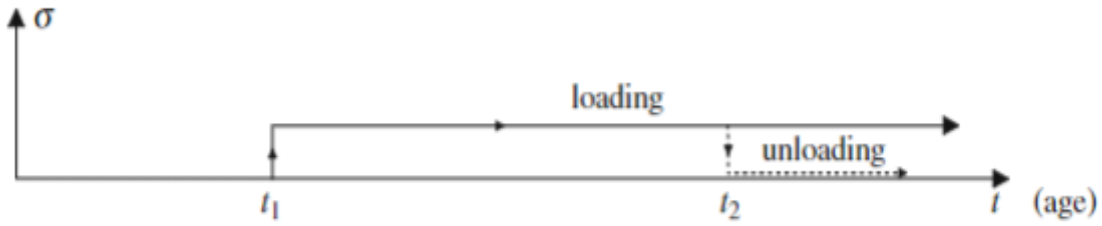

b)

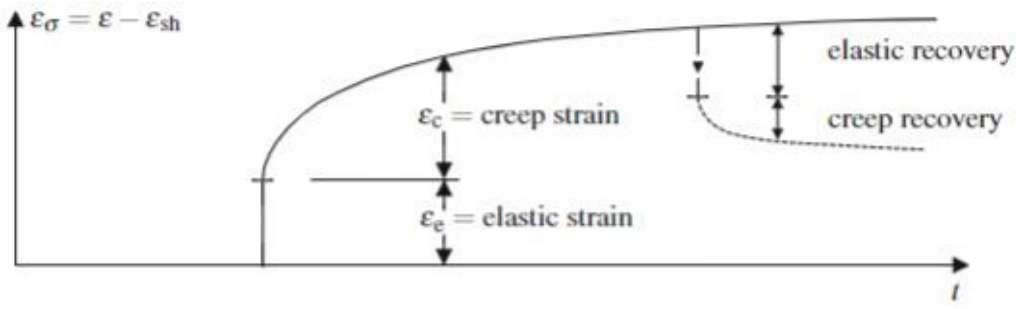

Figure 4: Curves of concrete cylinders creep and recovery [Bazant, 2018].

2.4.1 Concrete Material Level Creep

Concrete is one of many materials that experience the time-dependent deformation known as creep. This behavior is extremely important when considering the effect that a sustained load has on a concrete member. To fully understand the creep effect, a firm knowledge of what is happening at the material level of concrete is needed.

At the material level, the cause for creep strain is the “breakage and reformation of atomic bonds at various highly stressed sites within the colloidal microstructure of the calcium silicate hydrate gels in the hardened cement paste” [Bazant, 2018]. In simpler terms, concrete can adapt to levels of high stress inside the microstructure of the

hardened cement paste by breaking at these high stress points and reforming these bonds after the load is more evenly distributed. This breaking and reformation produces strain in the direction of loading on the specimen. This mechanism of creep generally occurs at service load levels (<0.4f'c).

There are three stages of concrete creep: primary, secondary, and tertiary creep (Figure 5). Primary creep is the early creep behavior when large amounts of strain occur with respect to time. This rate steadily decreases and eventually levels out to a more constant rate; this is Zone I in the figure below. Secondary creep is the portion of the graph (Zone II) when the rate of creep is constant in low to moderate loading cases and linear in higher loading cases. Tertiary creep (Zone III) occurs only in concrete loaded at or above 0.8f'c; it is at these high levels of loading in which the creep rate may begin increasing after secondary creep occurs. This acceleration is caused by propagation of microcracks inside the cement microstructure.

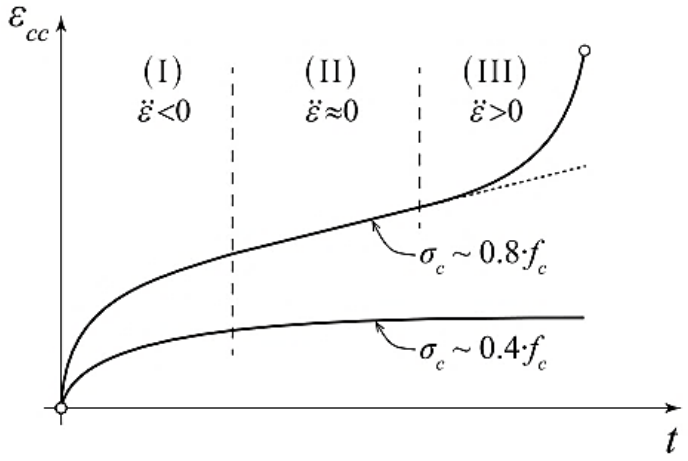

Figure 5: Standard shapes of strain vs. time curves of concrete creep.

In theory there is no limit to creep strain; the process of redistributing the load amongst the microstructure of the concrete will occur if the stress is applied [Bazant, 2018]. While

it may seem alarming that concrete members continue to strain indefinitely, at low to moderate stresses, creep strain rates gradually decrease with time. At these low to moderate stresses, measurable creep strain basically ceases in a period of two to five years. In this time period, the creep strains can be on the order of one to three times the instantaneous elastic strains.

2.4.2 Characteristics that Impact Creep Behavior

As concrete is variable by nature, components that traditionally are used to design the strength of the concrete are also linked to how the concrete will react under a sustained load. These components include the age of the concrete, the level of stress applied, the water cement ratio, and the moisture content of the atmosphere. Small changes in the properties of each component can greatly affect the specimen's creep behavior.

2.4.2.1 Aging

Concrete continuously experiences increases in both strength and its modulus of elasticity as it grows older – this is due to aging. Aging is a property of concrete that impacts its creep behavior. This process occurs when free water in the pores of the hardened cement continue to react with the tricalcium silicate over the entire lifetime of the concrete. This reaction produces tricalcium silicate hydrate gel that slowly fills the voids in the cement paste. As more voids are filled and the concrete becomes less porous, it gains more strength and stiffness.

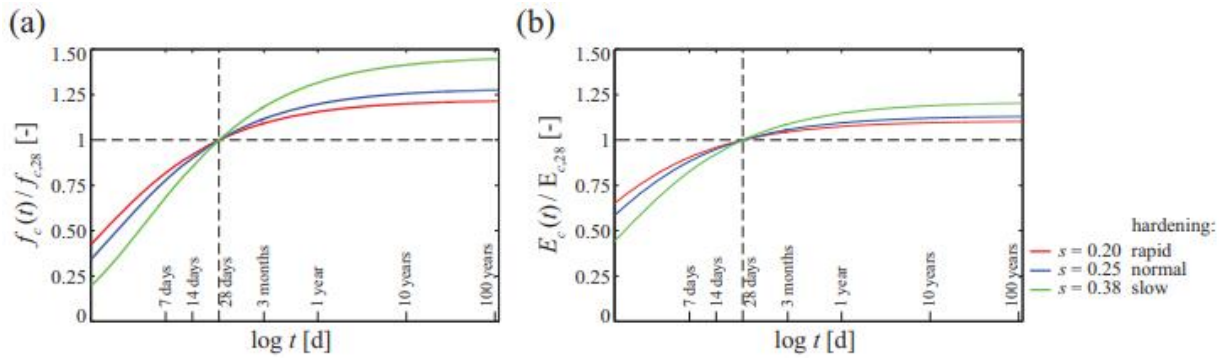

Figure 6: Development of concrete compressive strength (a) and concrete modulus of elasticity (b) with time [Tasevshi,2019].

The more time that concrete is given to age before stress is applied results in less creep strain. The development of the tricalcium silicate hydrate gel causes the cement microstructure to strengthen with time. This increase of hardened cement limits the breakage and reformation of the bonds when experiencing stress; thus, older concrete creeps less (Figure 7).

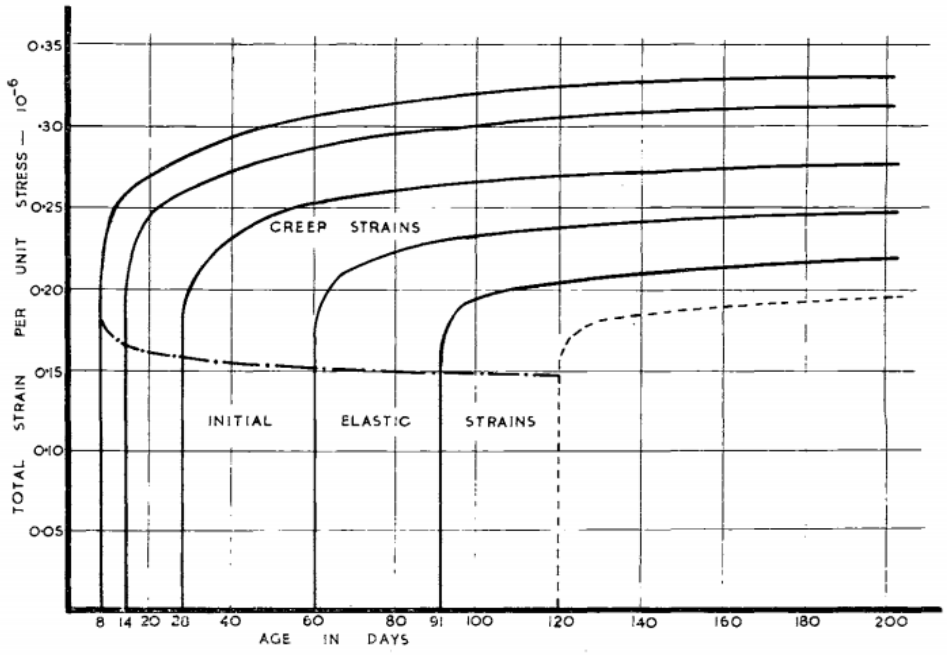

Figure 7: Strains due to constant load applied at various ages [Ross,1958].

2.4.2.2 Level of Stress

When loaded in compression, the rate of creep is largely determined by the amount of stress applied to the concrete specimen. This proportionality applies up to about 40-50% of the ultimate strength of the concrete [Illston,1965]. After 40% strength, microcracks begin to form between the bonds of hardened cement particles and the aggregates. These microcracks indicate a transition out of the elastic deformation portion of loading and into plastic deformation. The presence of microcracks can cause both nonlinearity in creep behavior and increased strain rates.

Plain concrete specimen that are loaded in tension have a similar reaction to increased levels of stress applied. Figure 8 shows three different concrete specimens loaded at different stress levels in a uniaxial tensile test. The specimen loaded at 25% of the ultimate strength (59 psi) and the specimen loaded at 50% of the ultimate strength (122 psi) exhibits similar creep behavior in the period of 110 days. The specimen loaded at 75% of the ultimate strength (171 psi) has large increases in creep strain throughout the test. While it is plotted on the same time axis as the other two, the 75% specimen experiences failure due to creep strain after 24 days of loading.

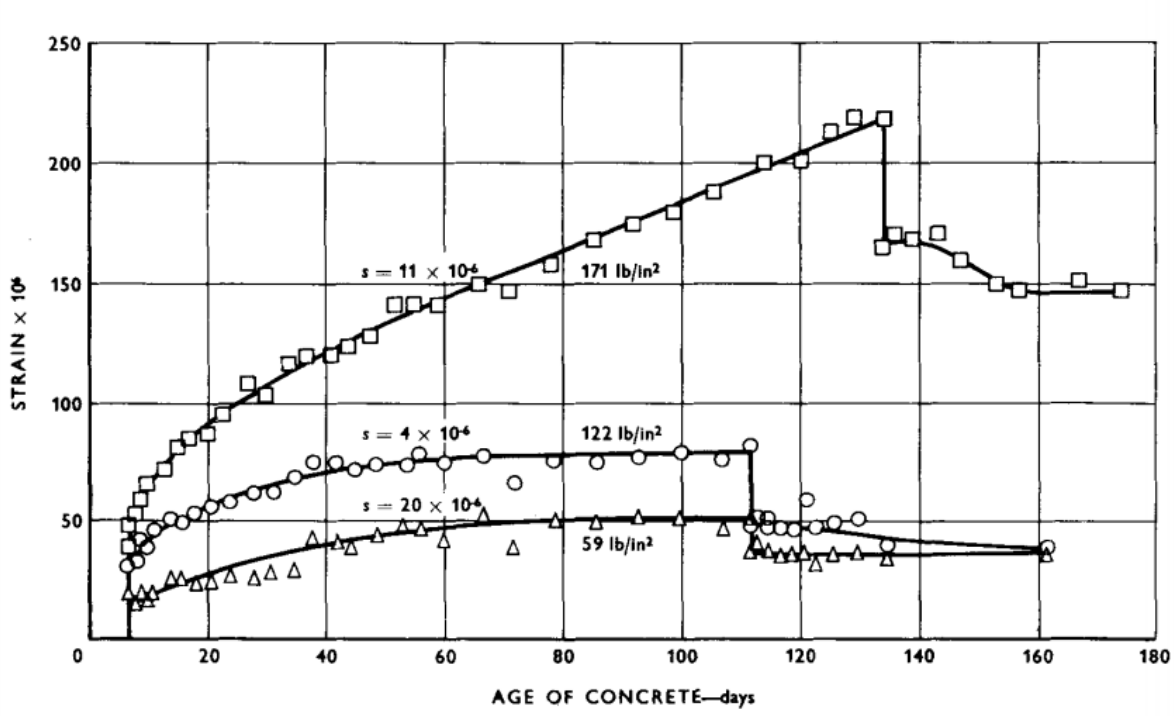

Figure 8: The effect of the level of tensile stress on the creep strain of concrete [Illston,1965].

2.4.2.3 Water-Cement Ratio

Mixing water and cement activates a reaction between the two materials that eventually hardens and bonds the aggregates in the mix together. This reaction between cement and water is known as hydration. Besides acting in the hydration reaction, water also makes concrete fluid enough so it can flow and fill formwork without too much difficulty; this is a property known as workability. The amount of water that is needed to properly hydrate and harden the concrete is much less than what is needed to create a workable concrete [Wight,2009]. The excess water creates voids in the hardened concrete which both weakens it and causes an increase in creep strain. Numerous voids create more

opportunity for high stress concentration in the cement microstructure which leads to an increase in creep strain.

While the relationship between adding more water and the resulting increase of creep is straightforward, adding cement to a concrete mix tends to increase the creep strain while also strengthening the concrete. Concretes with the highest percentage of cement will creep the most because cement microstructures, not aggregates, are responsible for creep behavior [Wight, 2009]. Therefore, having a higher percentage of cement in a mix results in a larger creep strain. This property is interesting because generally speaking, higher-strength concrete creeps less than lower-strength concrete. In this case, increasing the cement content tends to strengthen concrete and increase the creep strain.

2.4.2.4 Humidity

The time-dependent components of shrinkage and creep are intertwined. While the amount of moisture in the atmosphere directly relates to the amount of shrinkage strain (Figure 3), this factor also affects the creep strain rate of plain concrete once stress is applied. Exposing a specimen to an atmosphere of less than 100% humidity causes the cement paste micropores to begin to dry out. This drying phase produces local stress peaks in the calcium silicate microstructure. With additional stress applied to the concrete, the rate of cement bond breakage accelerates (as does the amount of creep) [Bazant, 2018].

The micropore drying out process is not uniform throughout the cross-section of the concrete and thus, the stress peaks are not uniform either. An imbalance of peak stresses can lead to microcracking. This microcracking releases stress at the peaks in order to

reach a state of equilibrium between levels of high and low stresses. Microcracking increases the shrinkage of the concrete by allowing the concrete to compress more. This increase in shrinkage due to microcracking is referred to as true shrinkage.

The microcracking caused by the uneven drying of the inside of the cement also allows the concrete to creep more while the loads are being redistributed within the microstructure. Once a stress is applied, concrete will creep almost twice as much at 50% humidity then it would at 100% humidity [McCormic,2005].

2.4.2.4 Steel Content

As discussed previously, concrete undergoes time depended volume changes known as creep and shrinkage; steel, however, does not experience these changes in volume. As creep occurs in the concrete, steel reinforcement blocks it and picks up more and more load [McCormic,2005]. The fact that the steel carries the long-term stresses that accumulate due to creep results in a large reduction in the overall creep of the specimen. As a result, creep strains are smaller than they would be compared to a plain concrete member with identical stresses applied. However, in order for the steel to carry the stresses resulting from concrete creep, the bond between the steel and concrete must be able to transfer those stresses.

2.5 Effect of Concrete Creep on Strength

In laboratory settings, loadings can be applied in a manner of constant strain rate. This is quite unlike actual structures which are loaded relatively quickly and held constant for very long periods of time. Figure 9 shows the difference between these two loadings types. The constant load applied quickly and sustained leads to a lower strength than the specimens loaded at a constant strain rate.

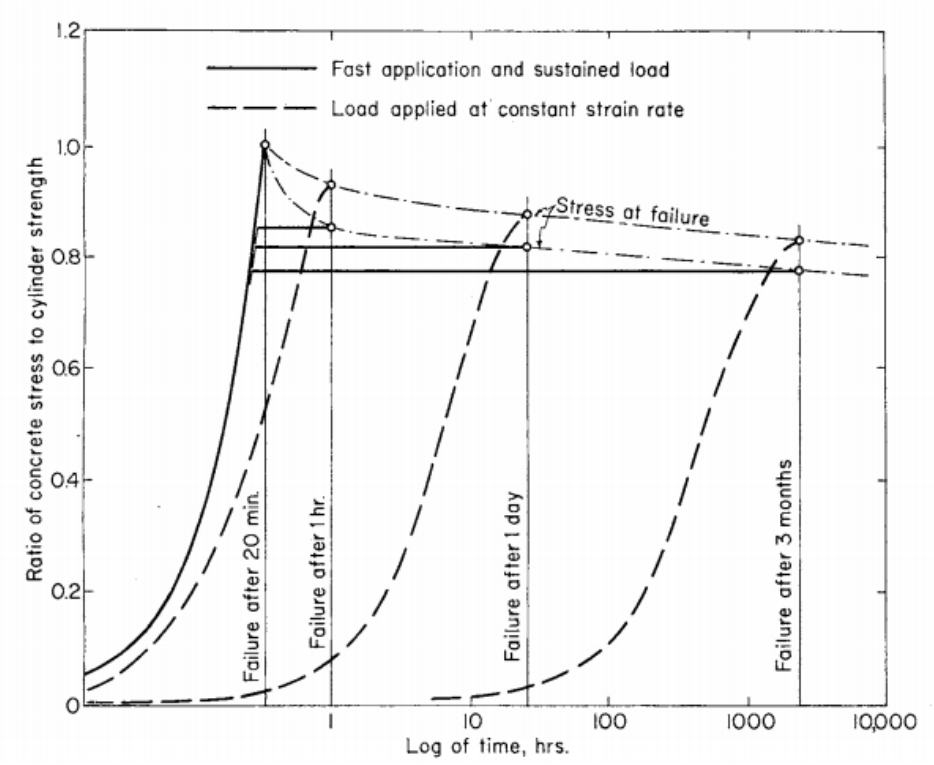

Figure 9: Reaction of ultimate strength on concrete compression tests based on loading rate [Rusch,1960]

If the degree of sustained loading is higher than the sustained load strength, the deformations of the concrete specimen could eventually accelerate and lead to delayed failure [Figure 10]. If the degree of sustained loading is less than the sustained load strength, the specimen will stabilize and approach a limiting strain value. The sustained

load strength of normal strength concrete is about 75-80% of the strength in a short time test [Rusch,1960].

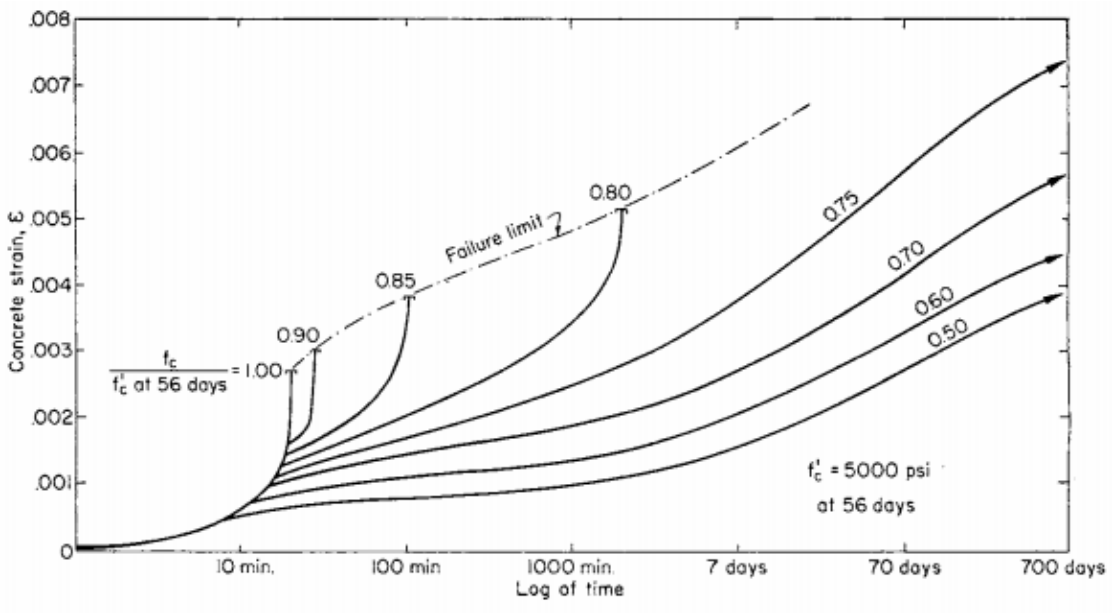

Figure 10: Strains under sustained load

Sustained load strength decreases as load duration increases. Specimens loaded past the 75-80% threshold experience decreasing ultimate strengths. This relationship, denoted as the "Failure limit" in Figure 11, illustrates this reduction of strength as duration increases. The elastic modulus of elasticity (E_c) is the straight line in the figure below; this represents an elastic linear stress/strain relationship that the specimens are expected to follow at extremely short load durations. The modulus of elasticity decreases as the load duration increases. The limit to this slope decreases is denoted as the "Creep limit". This creep limit occurs at a hypothetical infinite loading duration that eventually reaches the failure limit. By being confined to the left by the elastic modulus of elasticity, to the right by the creep limit, and on top by the failure limit, all possible relationships of stress and strain are enclosed [Rusch,1960].

The previous figures are on plain concrete. The behavior of reinforced concrete, where the reinforcement is able to carry some of the stresses caused by concrete creep, is less well-known. Therefore, this research project is focused on assess this behavior and this thesis specifically looks at the bond of the reinforcing bar to the concrete.

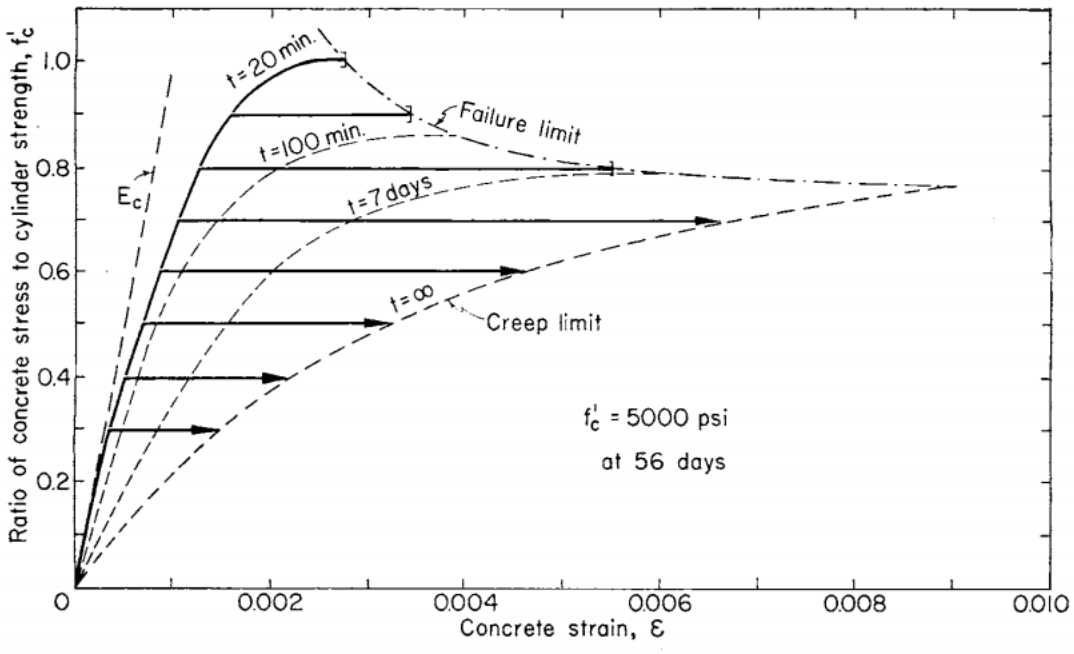

Figure 11: Influence of load intensity and duration on concrete strain [Rusch,1960]

2.6 Bond Between Concrete and Reinforcing Bar

2.6.1 Bond Stress

The basic theory of a reinforced concrete member is combining the two materials in order to maximize the efficiency of both. A well-designed concrete member relies on the concrete to carry the compressive forces, while the steel takes the tensile load. For this to work, there must be a transfer of these forces between the two materials; this force

transfer is known as bond. When a force is applied to the reinforcing bar, bond stresses must exist in the opposite direction in order to keep the system in equilibrium (Figure 12). Once bond stresses stop acting on the system, the bar pulls out and the beam fails [Wight, 2009].

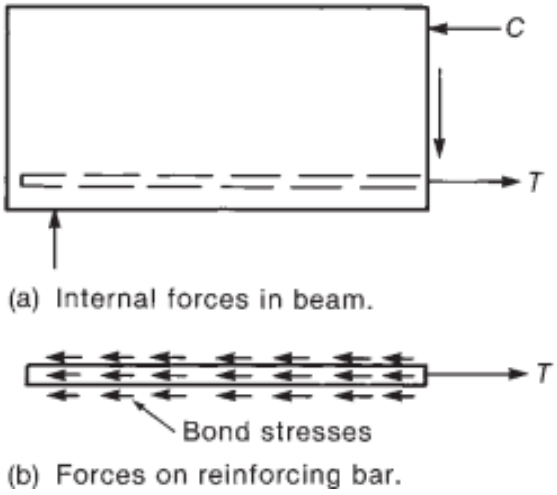

Figure 12: Bond Stresses developing in a RC member [Wight, 2009].

The actual mechanism behind bond includes three separate components: the chemical adhesion between the cement paste of the concrete and the steel of the reinforcing bar, the friction due to shrinkage of the concrete, and the mechanical interlock of the system [Rao,2007]. Plain reinforcing bars do not have the mechanical interlocking bond, so it only experiences the first two components. Deformed reinforcing bars have ribs in order to increase the mechanical interlock between concrete and metal; this interlocking bond is much greater than both chemical adhesion or friction bonds. This causes the other two mechanisms of bond to act as smaller, secondary effects in deformed bars [Walker, 1997]. As deformed bars are used in the majority of reinforced concrete members, this interlocking bond is the main mechanism in developing bond stresses in most cases.

Transferring the force in the steel bar to the concrete using these ribs creates two components acting on the concrete: longitudinal and radial forces (Figure 13). The longitudinal component acts parallel to the reinforcing bar and bears against the concrete touching the front face of the rib. The radial component acts transverse to the ribs; this component causes tensile stresses wrapped around the reinforcing bar [Mazumder, 2014].

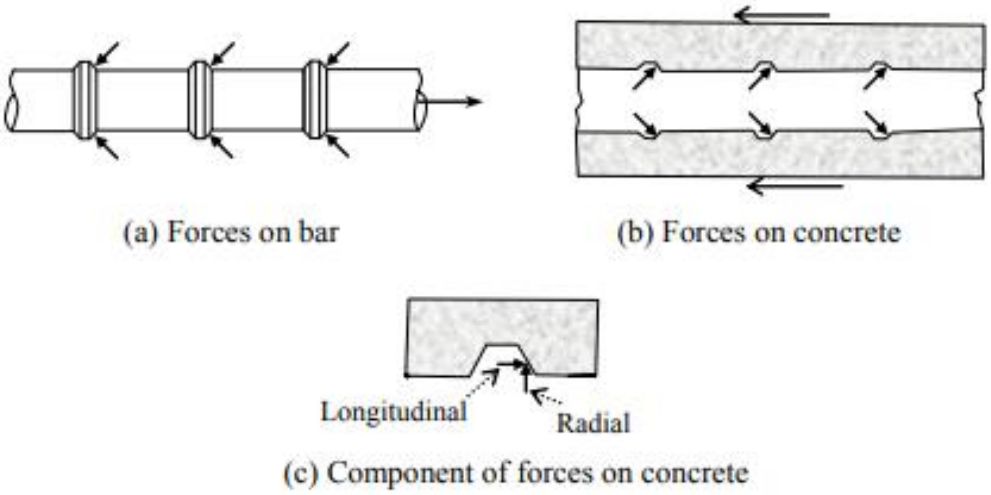

Figure 13: Transfer of forces between steel and concrete [Mazumder, 2014].

2.6.2 Bond Stress Distribution

True bond stress distributions are not constant throughout RC members. In places where cracks occur concrete is unable to carry load, so the bond stress at that location goes to zero; the steel at these crack locations are responsible for carrying the entire load. Between cracks, the bond stress develops based on the expression based on the applied force, f_s,

$$\frac{df_s}{dx} = \frac{4u}{\mathrm{d_b}} \tag{2.1}$$

where u is the true bond stress acting in the length dx and d_b is the diameter of the reinforcing bar [Wight, 2009]. The array of different lengths between cracks causes different size concrete and steel stress distributions along the length of the member (Figure 14). For a single reinforcing bar subjected to tension, the following equation is used to calculate the bond stress.

$$u = \frac{T_c}{\pi d_b l_d} \tag{2.2}$$

where T is the axial force on the bar, l_d is the bonded length, and d_b is the diameter of the reinforcing bar.

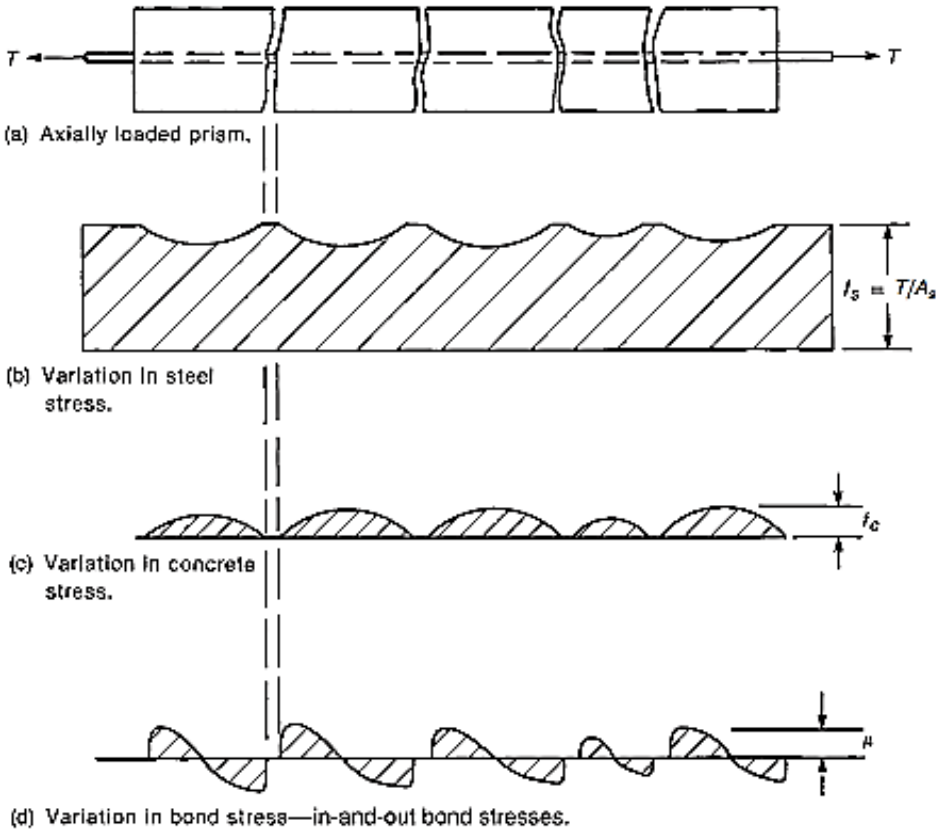

Figure 14: Variation of steel, concrete, and bond stresses throughout length of an axially loaded RC member [Wight,2009].

2.6.3 Factors affecting Bond Strength

When exploring bond strength, it is important to look at individual factors that may affect the strength of the bond. These factors include:

- Aging
- Tensile Strength
- Cover Depth
- Confinement
- Bar Size

Aging is always an important parameter in reinforced concrete. As previously discussed, aging is the property that causes concrete to gain strength with time. Unsurprisingly, gaining strength also results in higher bond stress development; concrete's tensile strength is a main component of the amount of bond stress it can withstand [Rao,2007]. Ribs on the reinforcing bar create tensile zones within the concrete; if the concrete can withstand a greater amount of tensile stress before cracking, the bond strength increases.

Besides aging, other factors that influence the tensile strength of concrete include w/c ratio, cement content, and type of aggregate. As it is so important in determining bond strength, measuring the overall tensile strength using a splitting tensile test is one of the most accurate ways to predict the bond behavior of concrete (Figure 15). However, as tensile strength of a concrete mix is almost always 8-15% of the compressive strength [Wight,2009], simple compression tests are also an efficient way to determine the bond strength.

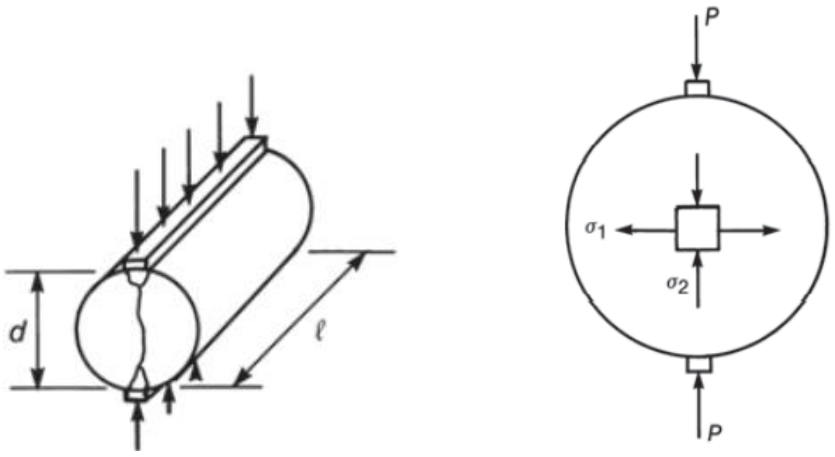

a) Splitting Tensile Test b) Stresses on element

Figure 15: Splitting Tensile Test and Resulting stresses on element [Wight,2009]

Cover depth is the distance from the reinforcing bar to the outside of the concrete specimen. As the amount of cover on the rebar increases, so does the confining pressure on that bar. The confining pressure makes it more difficult for cracks to open in the concrete; by reducing cracking, bond strength increases [Walker,1997]. While bond stresses increase with cover depth, there is a limit for this effect; the cover depth reaches a point in which the confining pressure's influence on developing bond stresses levels out. Figure 16 shows this relationship in terms of the ratio of the ultimate bond stress (f_{bu}) and the square root of the compressive cube strength of the concrete (f_{cum}) against the cover depth. In Figure 16, the "Bottom bar" has higher strength at the same cover depth as the "Top bar". As water rises to the top of concrete after it is cast, the top portion of the concrete naturally has an increased water-cement ratio and is slightly weaker.

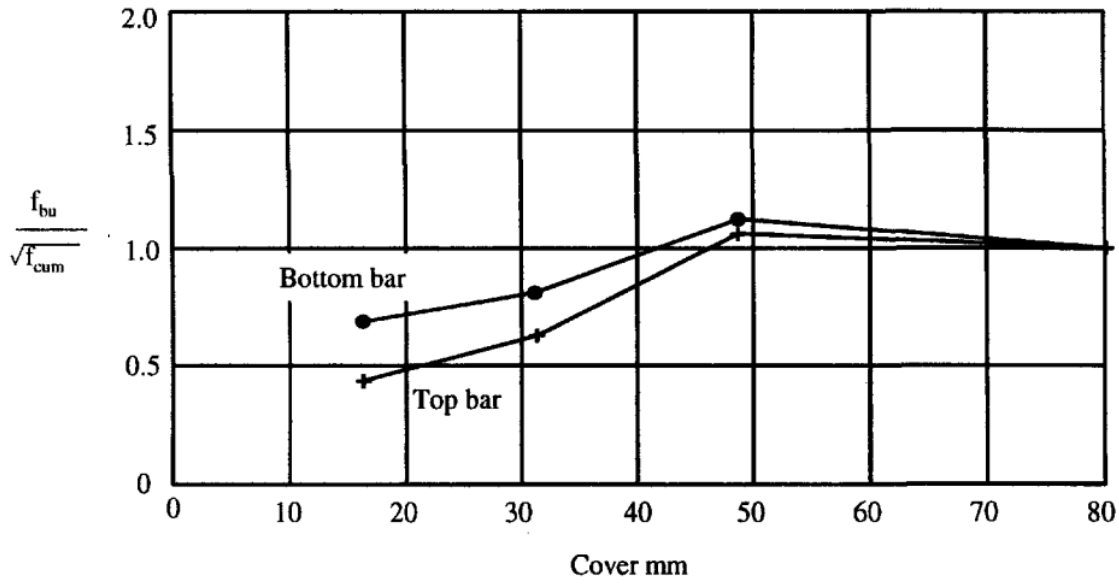

Figure 16: Relationship between the Bond Stress Ratio vs Cover Depth [Walker,1997]

The design of reinforced concrete cover depth is usually based on protecting the reinforcing bar from corrosion, not to provide adequate confining pressure to develop high bond strength. The American Concrete Institute (ACI) Code Section 4.3 has specific values of depth requirements for different bar sizes and conditions. These cover depths allow sufficient bond stresses to develop and thus designing cover depth can be simplified to standard depths found in the ACI Code.

Much like how more cover depth increases pressure around the reinforcing bar, confining stirrups act in a similar manner. As splitting cracks that form on the face of the reinforcing bar propagate outward, the development of these cracks can be resisted by confining stirrups. Concrete specimens in a pullout test with proper stirrup reinforcement experiences improved ductility [Figure 17]. The spiral confinement provides constant confinement throughout the length of the longitudinal bars which in turn allows for

greater confining pressure. The ties provide an adequate amount of confinement pressure, but comparably will always be less than the amount that spirals provide.

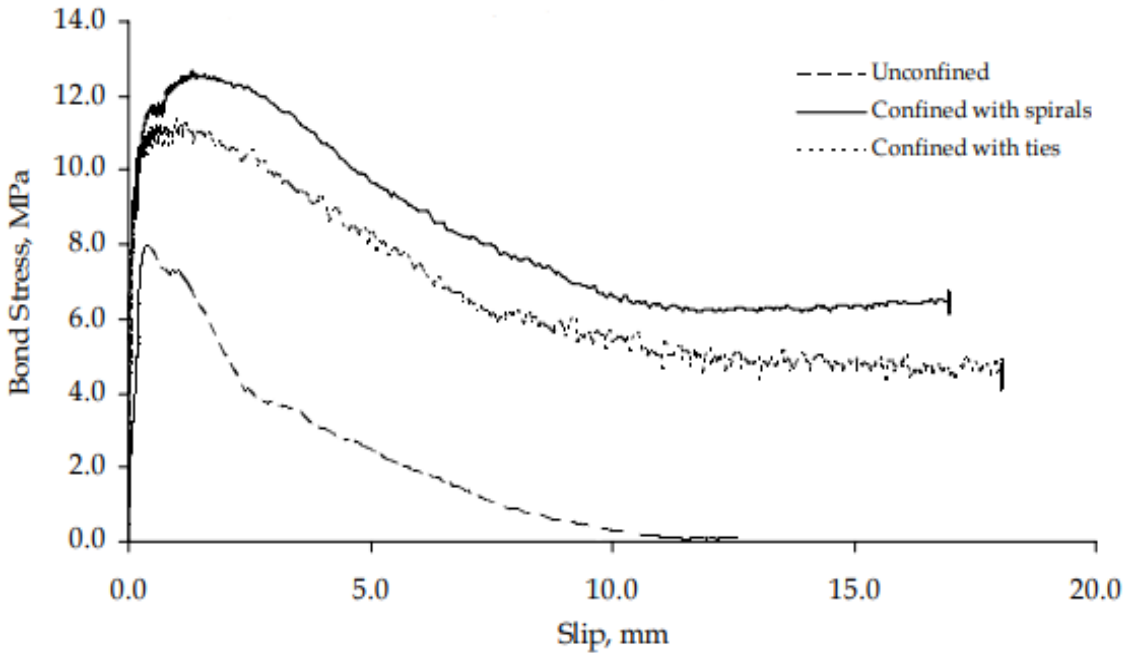

Figure 17: Typical Bond Stress vs. Slip for confined and unconfined pullout test specimens [Rao,2007]

The relationship between the size of reinforcing bar and the bond strength is important to consider. For a given bond length, with the same confinement pressure, larger bars reach higher total bond forces than smaller bars (Figure 18). One reason for this increase in bond strength is that as the bar size increases, so does the area in which concrete has to bond; an increase in bonded area results in higher bond strength. Larger bars also cause an increase in the effectiveness of transverse confining steel. As larger bars slip, higher strains and, thus, higher stresses are experienced throughout the concrete. These forces are mobilized in the transverse reinforcement which in turn provide better confinement.

The increase in bond force experienced by larger reinforcing bars results in the need for longer development lengths (bond lengths) in order for the steel to reach its potential bond force before failure occurs.

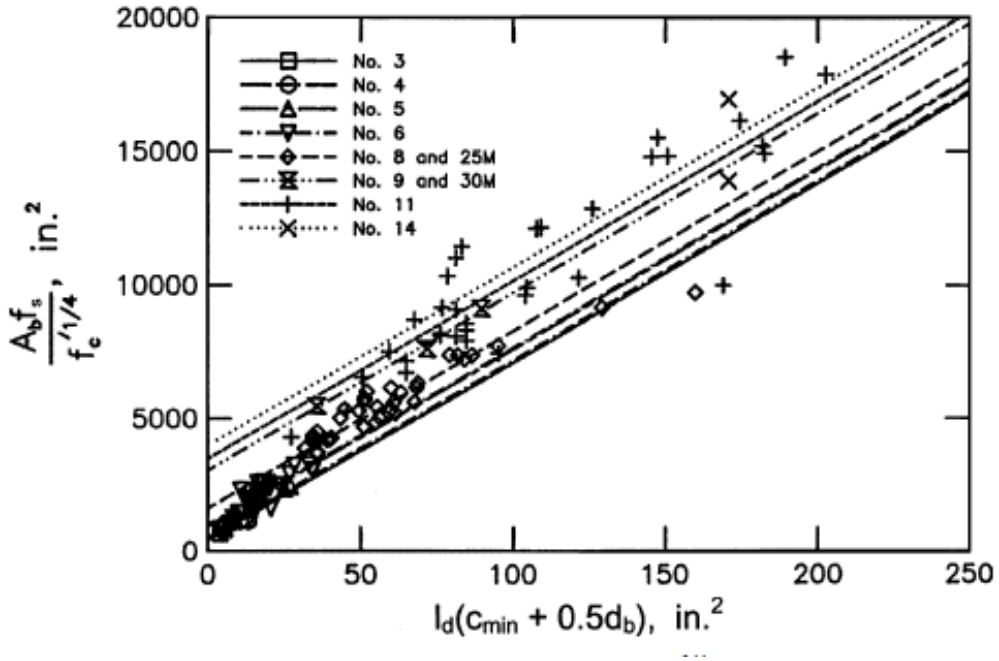

Figure 18: Bond strength of various sized reinforcing bar normalized with respect to $f_c'^{1/4}$ versus the product of the development length (l_d) to the minimum concrete cover (c_{min}) added to half of the center-to-center bar spacing [ACI 408,2003].

2.7 Crack Development Around Reinforcing Bar

2.7.1 Failure Methods

Applying a tensile force to a reinforcing bar embedded in concrete results in a transfer of that force to the concrete which mainly occurs at the vertical face of the ribs. As this force increases, one failure method occurs when the stress on the area of concrete touching the face of a rib becomes too great causing the concrete to crush. The other failure method that occurs is cone-shaped cracking that begins at the face of the rib and cracks transversely with respect to the reinforcing bar. It is not uncommon for both failure methods to occur simultaneously. The area in which crushing takes place and transverse cracks extend is known as the bond zone [Cox, 1998]. Deformation to the concrete in this bond zone impacts the bond strength of the composite material greatly.

2.7.2 Progressive Failure Stages

The type of deformation occurring to the concrete in the bond zone depends heavily on the level of stress that is applied. As the stress increases on a reinforcing bar subjected to a tensile force, the RC member experiences four main failure stages seen in Figure 19 below. Each of these stages have classifying characteristics that relate directly to the amount of stress applied to the system.

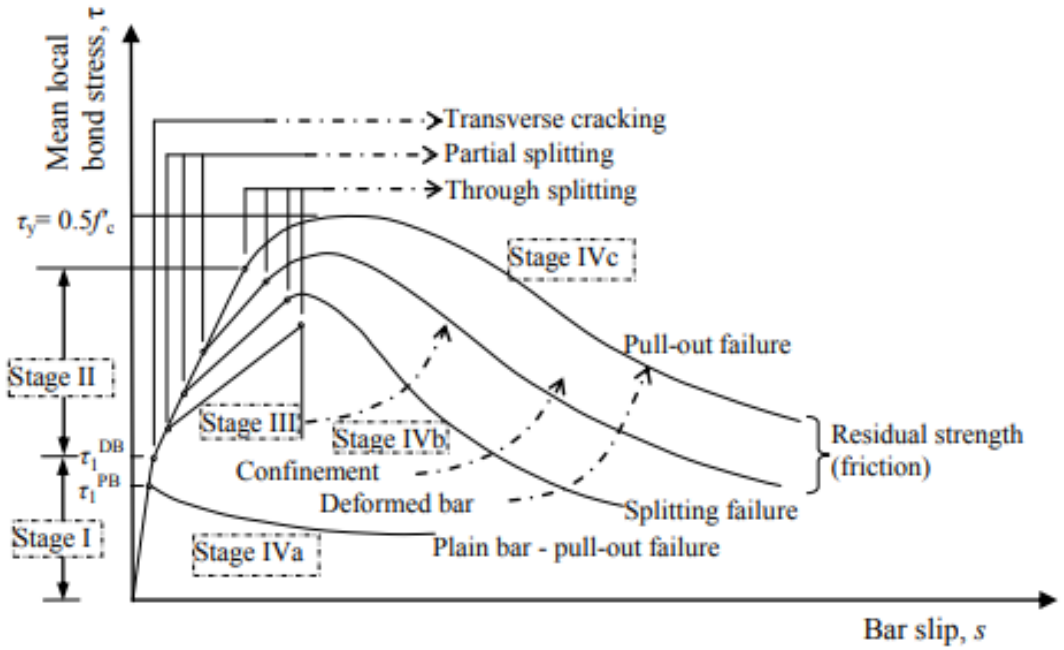

Figure 19: Typical stages of bond resistance for plain and deformed bar pull-out and splitting failure [Mazumder,2014].

2.7.2.1 Stage I – Elastic

The elastic stage occurs at low bond stress, when there is not enough force on the reinforcing bar to instigate any type of cracking in the concrete. As no cracking happens, this stage is characterized by a linearly-elastic respond to loading. This means that once unloaded, the specimen will return to its original shape with no permanent deformation.

The stress at this stage is low enough that cement adhesion to the reinforcing bar is still present. The adhesion is the main component in developing bond stress at this point which causes deformed and plain bars to behave similarity at this stage. The elastic stage will last until bond stresses are experienced that are greater than the adhesive bond between concrete and reinforcing bar [Mazumder, 2014].

2.7.2.2 Stage II – First Cracking

As the stress continues to increase on the embedded reinforcing bar, the concrete will begin to crack – thus entering the partially cracked-elastic stage. This stage is characterized by the chemical adhesion between the reinforcing bar and the concrete breaking down, as well as high bond stresses beginning to form at the ribs of the reinforcing bars. With increasing stress localized at these ribs, the concrete experiences transverse microcracking that begins at the local peak stress on each individual rib [Yoto, 1971]. The transverse cracks are usually accompanied by crushing of concrete in these peak stress zones, resulting in small conical cracks that begin at the reinforcing bar rib (Figure 20). The cracks propagate outward along the angle of inclination of the bar force [Mazumder, 2014]. This angle is usually about 60° measuring from the reinforcing bar; however, the angle changes as the concrete continues to deform under loading.

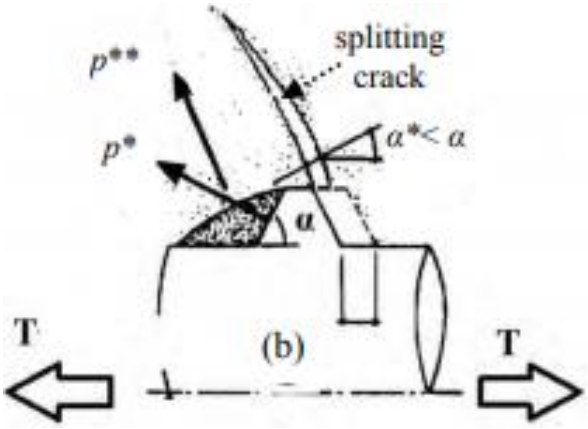

Figure 20: Formation of a splitting crack at rib face [Mazumder,2014].

2.7.2.3 Stage III – Plastic Deformation

Transverse cracks that first propagate to the surface of a concrete specimen are known as primary cracks. These primary cracks are actually smaller at the face of the reinforcing

bar and widen as they extend outward; this widening is caused by a loss of confining pressure. Not all transverse cracks formed at the face of the ribs extend to the surface of the concrete. In fact, the formation of these cracks is greatly influenced by surface deformations on the specimen [Yoto,1971]. The cracks that do not propagate are known as internal cracks. These cracks began to form in high stressed areas along the deformed reinforcing bar in Stage II; as more stress is applied, more of these internal cracks form. These cracks will point in the direction of the nearest primary crack (Figure 21). The formation of internal cracks indicates a tendency of discontinuity between the concrete and the reinforcing bar as increasing loads are applied. [Cox,1998].

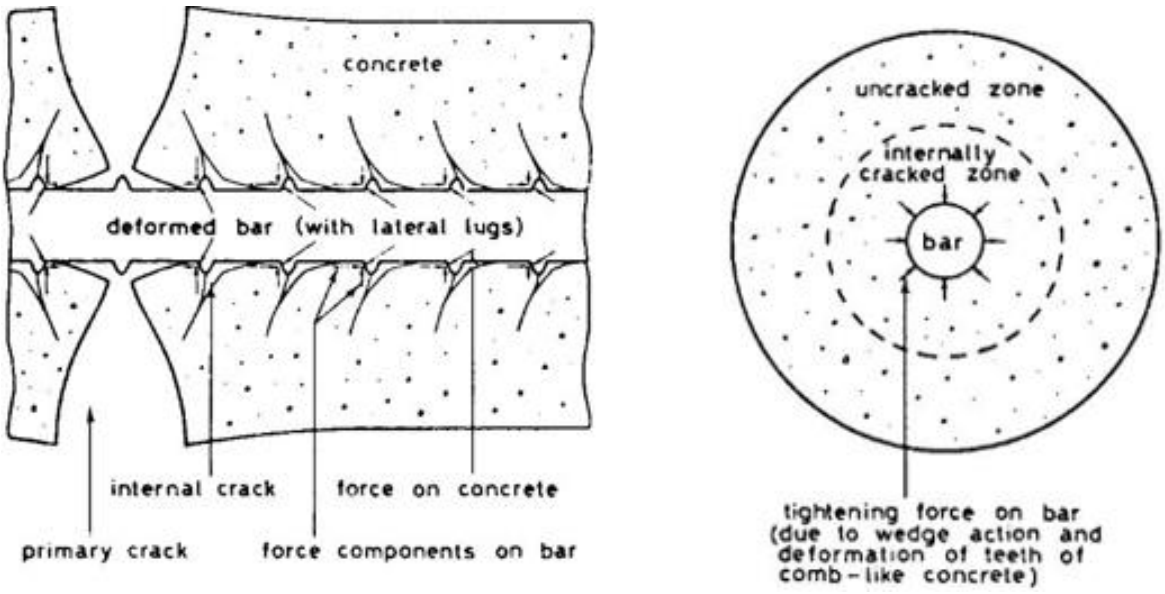

Figure 21: Formation and orientation of primary and internal cracks inside the bond zone [Yoto,1971].

Once the bond stresses become quite high, secondary cracks can appear at the surface of the concrete. These secondary cracks are oriented transversely to the reinforcing bar much like the primary cracks. However, while the primary cracks extend to the surface of the concrete at about a 90° angle, the secondary cracks begin as internal cracks formed at

about 60° and change to 90° angles as they near the surface of the concrete. Secondary cracks will usually form under a surface deformation where, in the cross-section, the concrete is weakest.

As stresses continue to increase, more plastic deformation occurs as longitudinal cracks (parallel to the reinforcing bar) begin to form. These longitudinal cracks form as concrete, on the compressive side of the rib, crushes which produces a wedging action that results in the angle of inclination of bar force to increase (*p***,Figure 20). This change in angle allows the radial component of the resultant force (Figure 13.c) to increase around the perimeter of the bar. In order to contain this radial pressure, concrete exerts confining hoop stresses on the bar [Mazumder,2014]. Stage III ends as the radial pressure overcomes the confining pressure allowing longitudinal cracks to propagate throughout the specimen.

2.7.2.4 Stage IV – Failure

As more longitudinal cracks progress throughout the bond zone, confining pressures weaken allowing cracks to widen and grow. The post-peak bond stress softening response from this type of cracking may fail due to pull-out failure or splitting failure (Figure 19). Pull-out failure occurs when the specimen loses the ability to have strong mechanical interlocking forces as the confining pressure weakens due to cracking. The diminished bond stresses are unable to resist the applied tensile force and the rebar pulls out of the concrete. A splitting failure occurs as concrete suddenly breaks apart due to the abrupt propagation of cracks. Splitting failures are oftentimes more sudden and thus have less of a softening response before failure (Figure 19).

Chapter III TEST SETUP

3.0 Experiment Overview

In order to study bond behavior at high sustained loads, a modified ASTM A944 beam-end specimen is used in this test. The test setup for these specimens is designed to allow a large tensile force to be applied to the test bar and held nearly constant. The design of the specimen, the design of the test setup, and the material properties of the specimen are given in this chapter.

3.1 Specimen Design

This experiment uses ASTM A944 beam-end test specimens in order to test the time-dependent characteristics of the concrete and reinforcing steel bond at high-sustained loads. This type of bond test, according to ACI 408, best replicates the state of stress in a standard RC bending member. By having the compressive reactions located away (at least a distance of the embedment length), the bonded reinforcing bar and surrounding concrete are placed directly in tension.

The specimen consists of a test bar that is cast into a reinforced concrete block measuring 24 in long by 8 in wide by 16 in high (Figure 22). Each specimen is reinforced with four closed steel stirrups made with bent #3 deformed reinforcing bar. These stirrups are oriented parallel to the test bar and are held in place by #3 bars oriented perpendicular to the test bar. The stirrups are parallel to the test bar so that they do not interfere with the bond properties. The perpendicular bars are located on the bottom half of the specimen – away from the test bar.

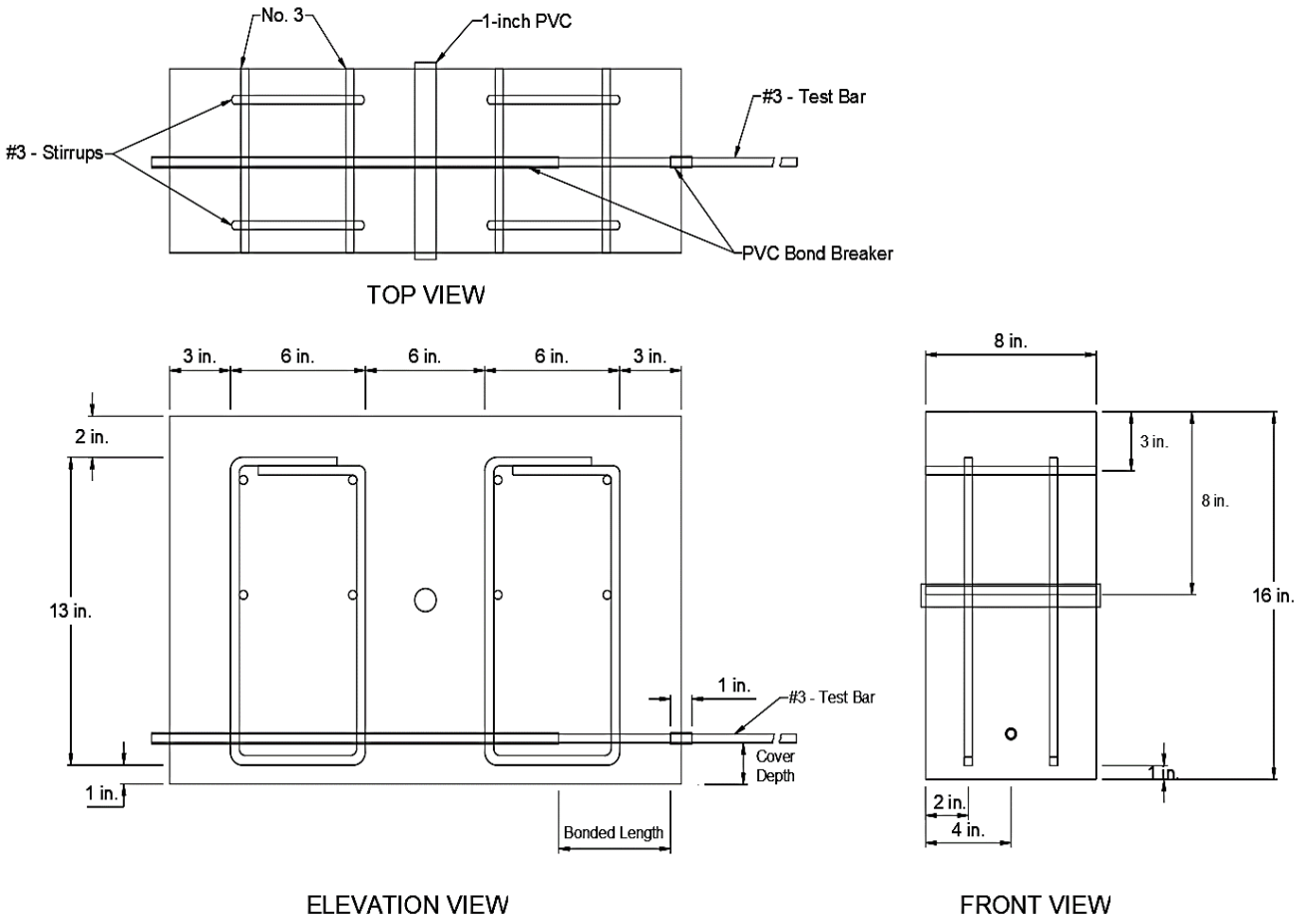

Figure 22: Design of the ASTM A944 beam-end bond specimen used in this test.

Each specimen contains 2 polyvinyl chloride (PVC) pipes which are used as bond breakers in order to control the bonded length of the test bar. Access to the free end (the end not loaded in tension) of the test bar is given by extending the longer PVC section (and the test bar) outside of the form. The smaller length (0.5 in) of PVC is placed at the fixed end in order to prevent a conical failure surface at the face of the concrete. The PVC pipes are cut at specific distances to ensure accurate bonded length. The cover depth is controlled by fixing the reinforcing bar at varying distances from the bottom of the form. The results of this design are bond specimens with precise embedment lengths at desired depths. The unbonding allows for lower tensile stress to be applied to trigger

failure; this, from a practicality standpoint, permits bond to be studied without high strength equipment.

One larger (1.0 in diameter) PVC tube is place through the center of the specimen to aid in moving the hardened concrete blocks. The concrete is cast so that the test bar was located at the bottom of the formwork (Figure 23 & Figure 24). The test specimens are moist cured for 7 days using plastic membrane covering and misted water in order to prevent rapid evaporation. The age of the first specimen tested (at the time it was tested) is about 6-months.

Figure 23: View of rebar and formwork pre-pour.

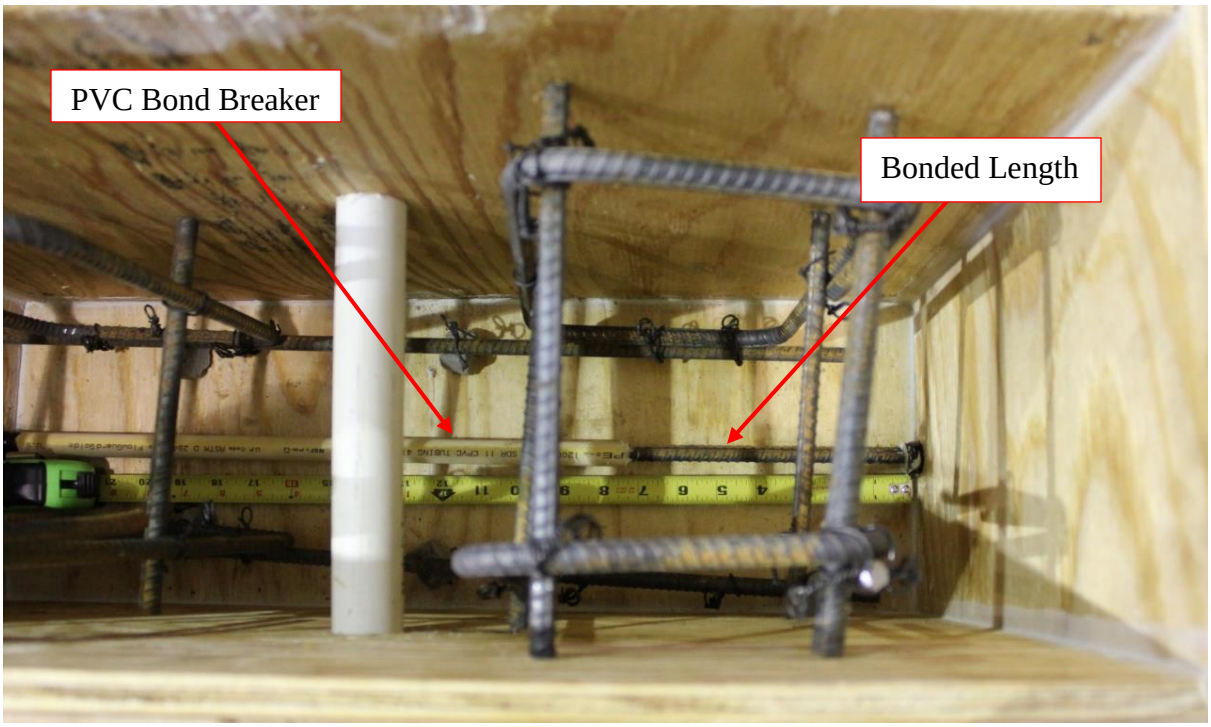

Figure 24: Close-up of concrete form and rebar placement.

3.2 Material Properties

This section provides the material properties of both the concrete and the reinforcing bar used in this bond test.

3.2.1 Concrete Material Properties

For the compressive strength test of the concrete, standard 4” x 8” cylinders were cast, capped, and tested until failure at the time of testing the control bond specimen. The average compressive strength and modulus of elasticity obtained from these compression tests were 5550 psi and 4000 ksi respectively (Table 1). The stress-strain curve of each

test is seen in Figure 25. A few of these same cylinders were tested in accordance with ASTM C946 to find the splitting tensile strength of cylinders. The average splitting tensile strength was 501.6 psi. An overview of this test setup and the failed specimens can be seen in Figure 26 & Figure 27.

Table 1: Material properties of concrete used in bond tests.

Average Compressive Strength of Concrete	**Average Splitting Tensile Strength of Concrete**	**Modulus of Elasticity of Concrete**
5550 psi	501.6 psi	4000 ksi

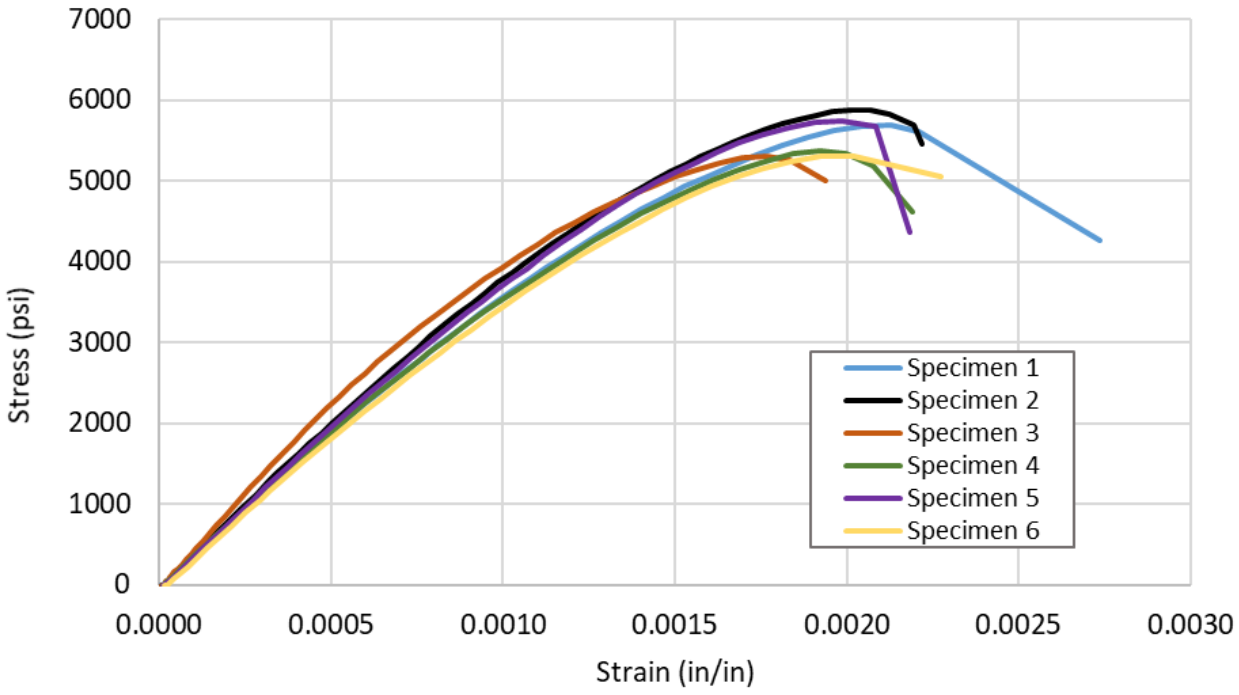

Figure 25: Stress vs. strain curves of uniaxial concrete compression tests.

Figure 26: Splitting tension test setup.

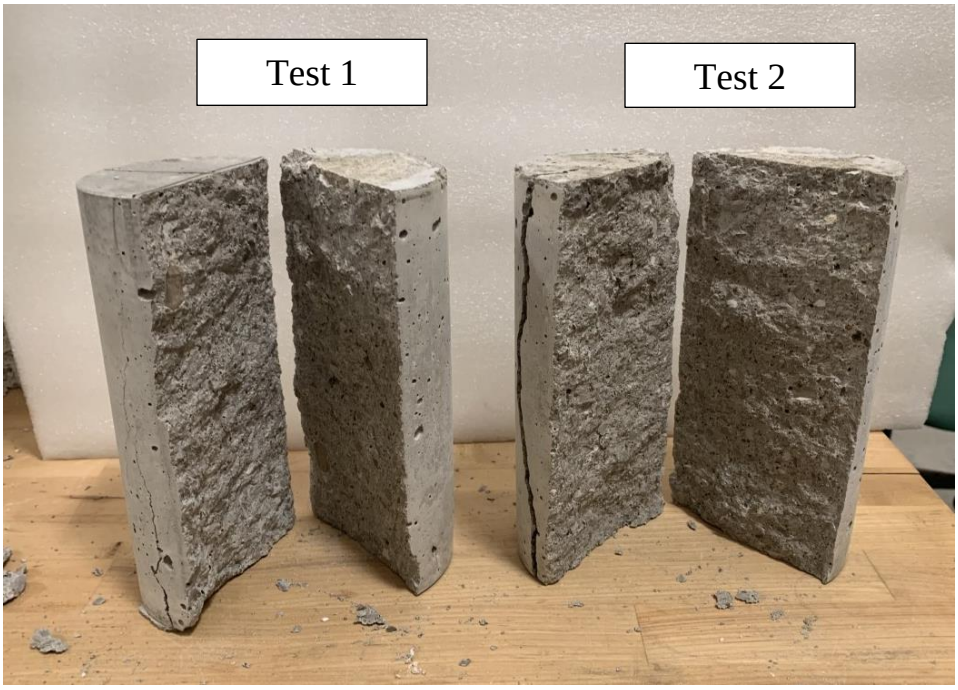

Figure 27: Broken splitting tension test cylinders.

Concrete Mix Design:

Date: 2/28/2020

Design Water: 77.5 gal

Design W/C: 0.459

Actual Water: 82.6 gal

Actual W/C: 0.487

Design Slump: 6”

Table 2: Concrete mix design quantities.

Material	Design Quantity (per yd^3)
3/8" Coarse Aggregate	1689 lbs
Sand	1400 lbs
Cement	564 lbs
Air entrainer	3.5 oz
Retarder	21.8 oz
Water	31 gal

3.2.2 Steel Properties

Samples of the #3 reinforcing bar, cut from the same bars used in the bond tests, were loaded uniaxially in tension until failure following the ASTM A370 procedure. The stress-strain curves of each test can be seen in Figure 28. The average yield strength for these reinforcing bars was 67.9 ksi while the average modulus of elasticity was 29,716 ksi (Table 3).

Table 3: Material properties of steel reinforcing bars used in bond test.

Average Yield Strength of Steel, f_y	**Average Modulus of Elasticity of Steel, E_s**	**Bar Diameter, d_b**
67.9 ksi	29716 ksi	3/8”

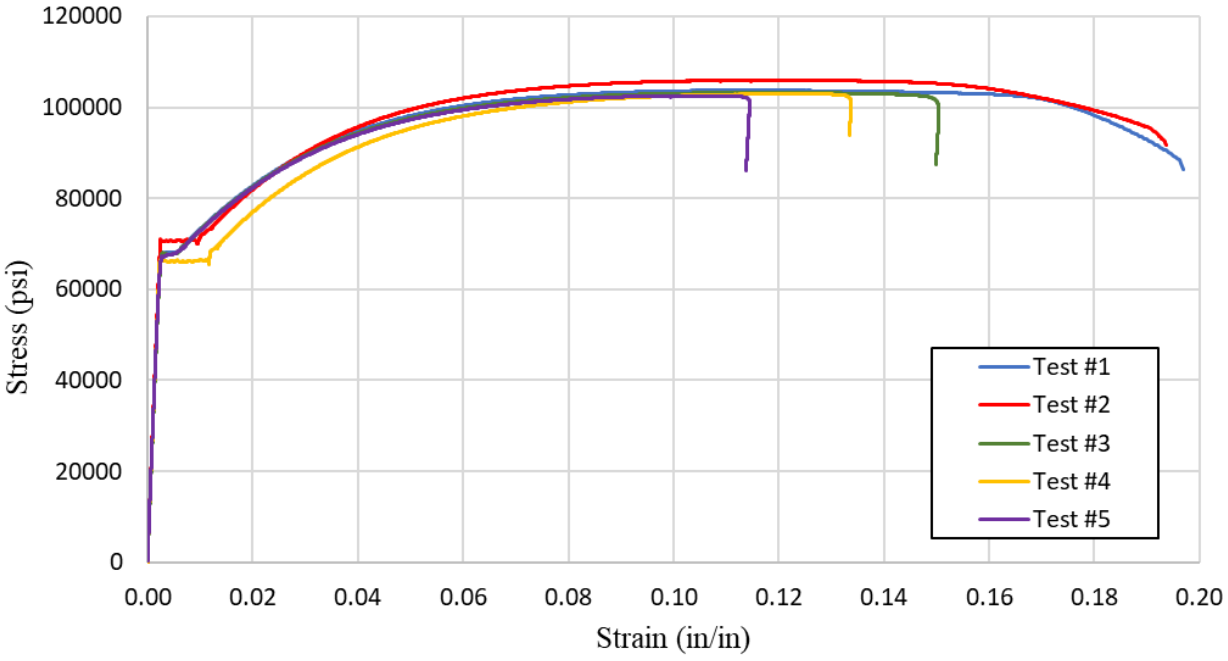

Figure 28: Stress vs. strain curve of uniaxial tension test of reinforcing bars.

3.3 Test Setup

The test setup complies with the requirements of ASTM A944 with modifications to enable long-term sustained loading. A drawing of the setup is shown in Figure 29.

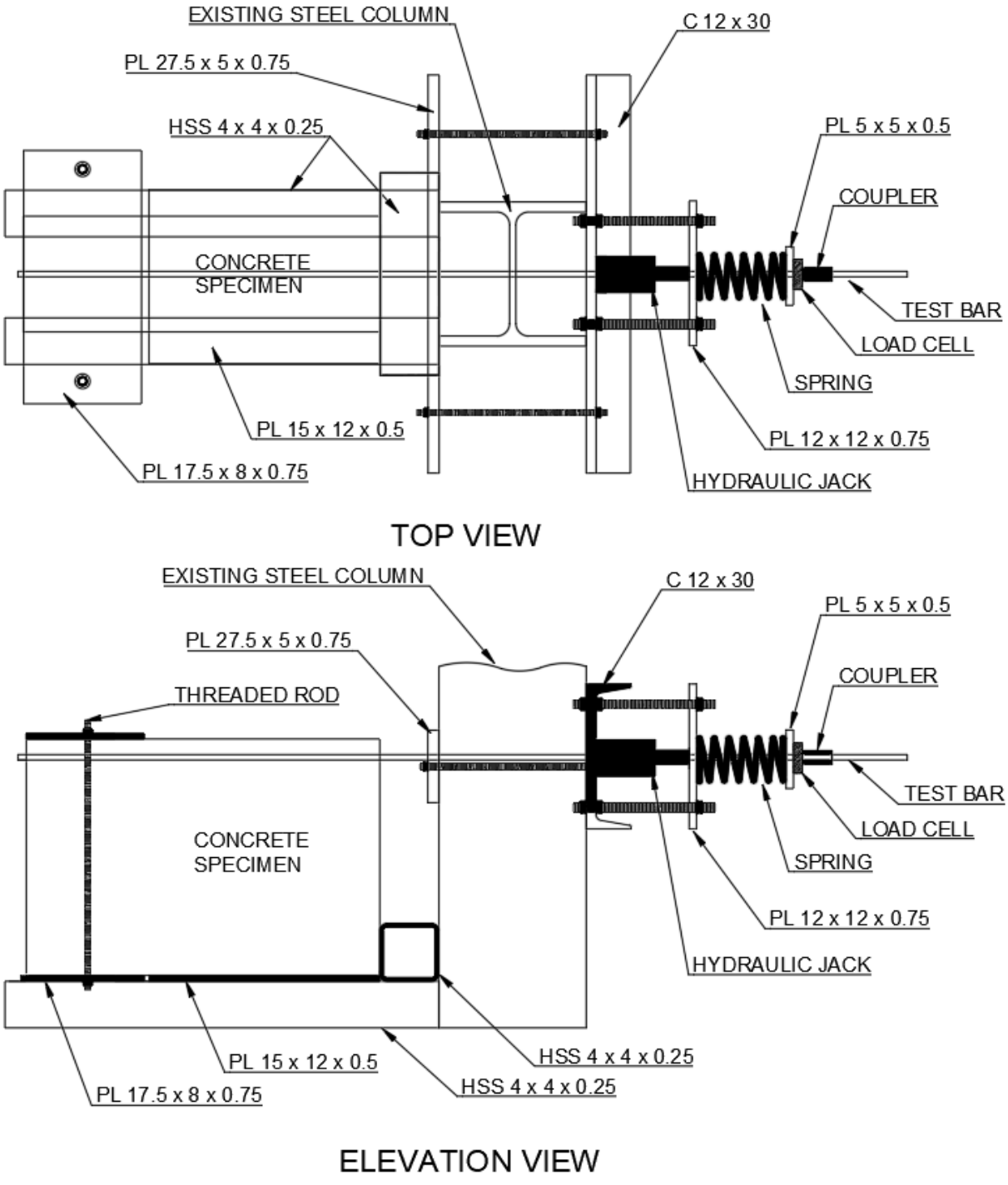

Figure 29: Design of the test setup.

The overall test setup is seen in Figure 30.

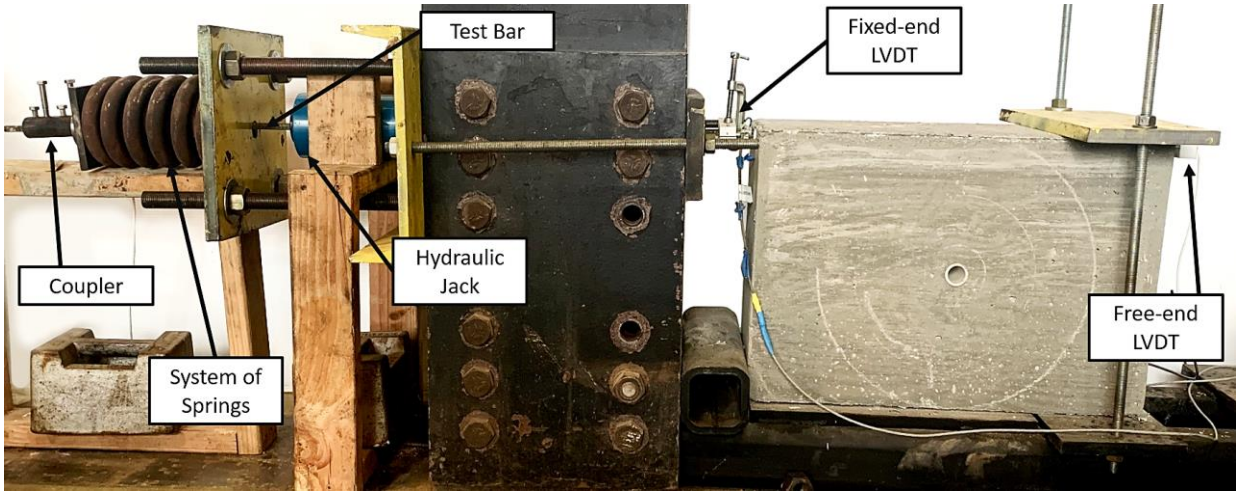

Figure 30: Overview of the test setup with a specimen in place ready to be loaded.

The hydraulic jack is pressurized which compresses the spring and loads the test bar in tension (

Figure 31). The compressed spring is used to help maintain an even force applied. The force on the bar is measured by a load cell located between the spring and the coupler. The coupler is used to grip the test bar at the far end and provide a reaction for the spring to compress against. This setup allows the test bar to be put under constant tensile force for long periods of time.

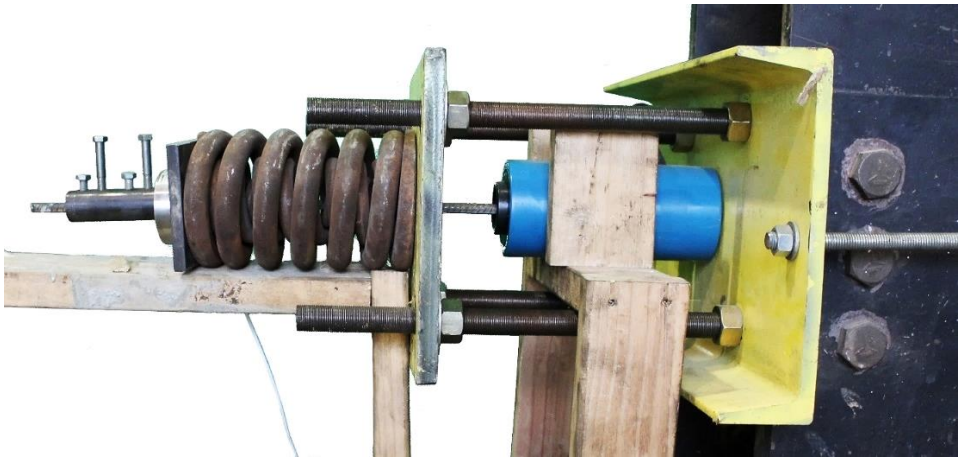

Figure 31: Loading configuration.

The free end of the specimen is held in place by a pair of steel plates attached with threaded rods and nuts. It is important that these plates are on far side of the free end so they can hold the specimen in place without causing a compressive force to the bond testing region. The second compressive force occurs at the base of the fixed end, again, away from the bonded length. These two compressive forces secure the test specimen so that a large tensile load can be applied.

Figure 32: Typical specimen ready to be loaded.

3.3.1 Test Instrumentation

Over the duration of loading, displacement of the test bar is measured at the free and fixed ends (Figure 32) of the specimen. In order to measure the slippage of the bar on the fixed end, two Linear Variable Displacement Transducers (LVDT), are attached to the bar on the front of the specimen. The average of these two LVDT’s slip readings is the amount of displacement the fixed end of the bar has in the direction of loading. Two

LVDTs are used to remove the effect of rotation of the bar on the LVDT reading. The free end slip is measured by a single LVDT which is pressed against the end of the bar on the rear of the specimen. The setup of both the free and fixed end LVDTs can be seen in Figure 33.

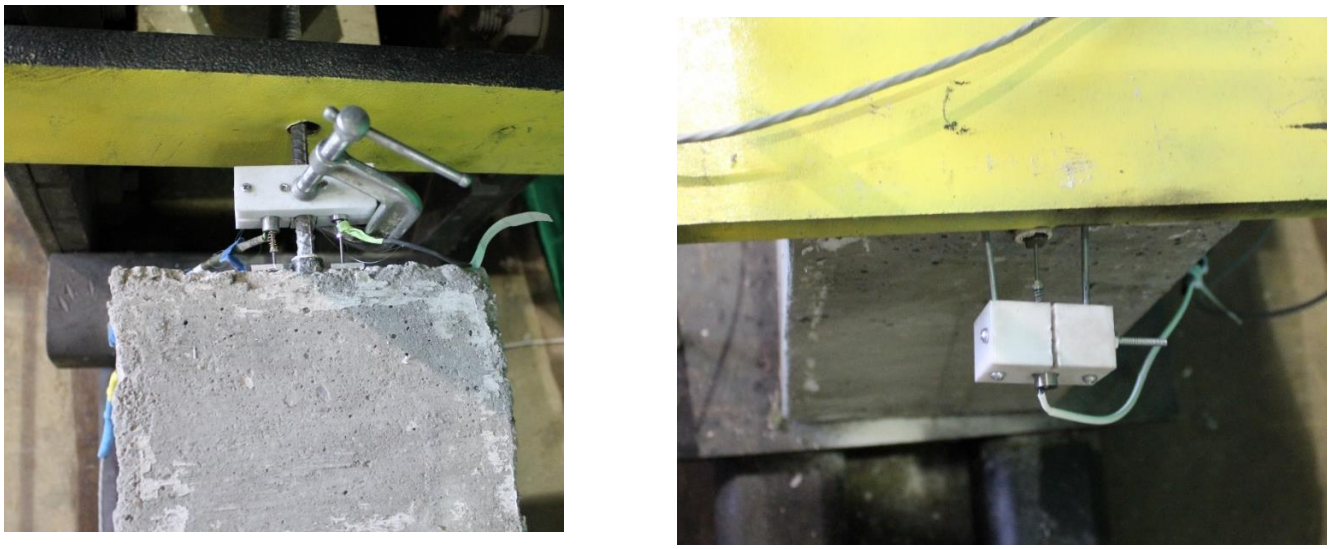

(a) (b)

Figure 33: (a) Fixed-end LVDT holder and (b) Free-end LVDT holder.

3.4 Test Matrix

In order to investigate the behavior of bond under high sustained load 25 beam end specimens were cast. Because the overall research program was using scaled specimens, the bond specimens were also cast with scaled properties (cover depth, concrete aggregate size, and rebar size). The original test matrix for the specimens is in Table 3.

The reference cover depth of 3/8” is half the typical cover depth for slab reinforcement (3/4”).

Table 4: Original test matrix (Number of specimens in ())

Bond Test Plan			
Length	**Thickness**		
	1/2"	3/8"	1/4"
3"	—	100% (1) 90% (1) 80% (1) +1	—
5"	100% (1) 90% (1) 80% (1) +1	100% (2) 90% (3) 80% (3) +1	100% (1) 90% (1) 80% (1)
7"	—	100% (1) 90% (1) 80% (1) +1	—

The nomenclature of labeling the tests is as follows: Test Name # (bonded length – cover depth) percentage of ultimate strength. For example, a sustained specimen with a 5-inch bond length and 3/8th -inch cover depth loaded to 90% of the expected ultimate strength is named: Sustained Test (5”-3/8”)90%. Unfortunately, due largely in part to the Covid 19 pandemic, only 3 sustained load tests were performed in time to be included in this thesis. The actual text matrix is seen in Table 5.

Table 5: Actual test matrix for thesis.

	Test Setup 1	**Test Setup 2**
Static Test	Control Test #1 & #2 (5" - 3/8") 100% (x2)	Control Test #3 (5" - 3/8") 100%
Sustained Test 1 & 2	Sustained Test #1 (5" - 3/8") 81%	Sustained Test #2 (5" - 3/8") 90%
	Began: 9/23/2020	Began: 11/6/2020
	End: 11/19/2020	End: in-progress
	Age at beginning of test: 196 days	Age at beginning of test: 233 days
Sustained Test 3	Sustained Test #3 (5" - 3/8") (96%)	
	Began: 11/20/2020	
	End: in-progress	
	Age at beginning of test: 247 days	

Two tests were conducted as control specimens. The loading was increased until failure of the specimen. The first two control tests were conducted on Test Setup 1; these two specimens had a nominal bond length of 5-inches and a cover depth of $3/8^{ths}$ of an inch. After testing these two, the first sustain load test, Sustained Specimen #1 (5" – 3/8"), was loaded to 81.1% of the average ultimate bond strength (6514-lbs) of the two static tests. The second sustained load test, Sustained Specimen #2 (5" – 3/8"), tested on Test Setup 2, was loaded to 90% of the expected bond capacity. The third sustained load test, Sustained Specimen #3 (5" – 3/8"), tested on Test Setup 1, was loaded to 96% of the adjusted expected bond capacity (6758-lbs). The capacity was adjusted based on including the sustained load capacity found after the first sustained load test in the average calculation. The expected load capacity will be adjusted throughout the remaining bond tests as a more refined capacity is gained with more specimens tested.

Chapter IV BOND TEST RESULTS

This section provides an in-depth look at the results of each bond tests and how well these results compare to what was expected.

4.1 Control Specimen Results

4.1.1 Control Specimen #1

While all the specimen tested for this thesis had a design bonded length of 5" and a cover depth of 0.375", the actual lengths and depths are slightly different between each specimen due to variability in construction. The first control test (seen in Figure 34) had an actual bonded length of 4.94" and a cover depth of 0.4095" (Table 6). This specimen was monotonically loaded until failure in order to determine the ultimate bond strength of these beam-end bond tests. Control Specimen #1 was made in a different concrete pour than the rest of the specimens tested; its strength value is 5211 psi (Table 6).

Table 6: Properties of Control Specimen #1

Actual Bonded Length, l_d (in.)	Actual Cover Depth, c_d (in.)	Compressive strength of Concrete used in Control Specimen #1 (psi)
4.94	0.4095	5211

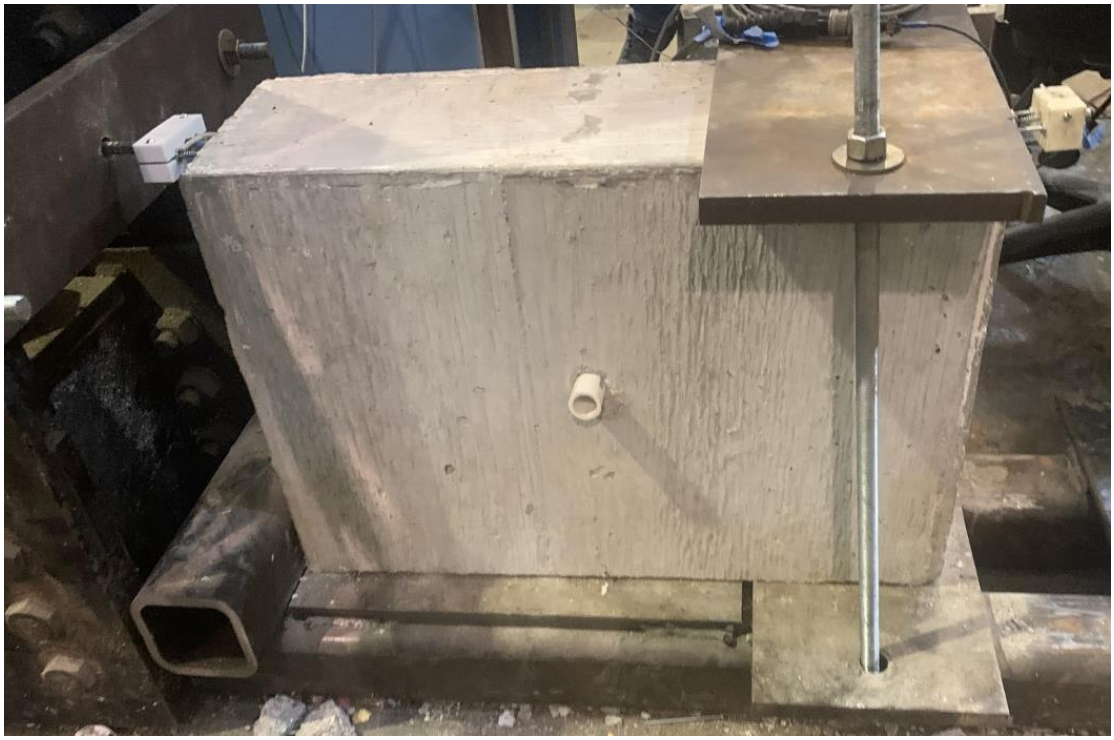

Figure 34: Control Specimen #1 prior to testing.

The sudden, brittle failure of this specimen indicates a splitting fracture. This was the expected mode of failure due to the specimens having small top cover, no transverse reinforcement, and thus minimal confining pressure. This type of failure is caused by hoop tensile stresses developing around the bar and causing cracks in the concrete (Figure 35 and Figure 36). Bond specimens with sufficient cover or transverse reinforcement will instead fail in a “pullout” failure mode. This type of failure occurs when the test bar shears the concrete along the top of the ribs.

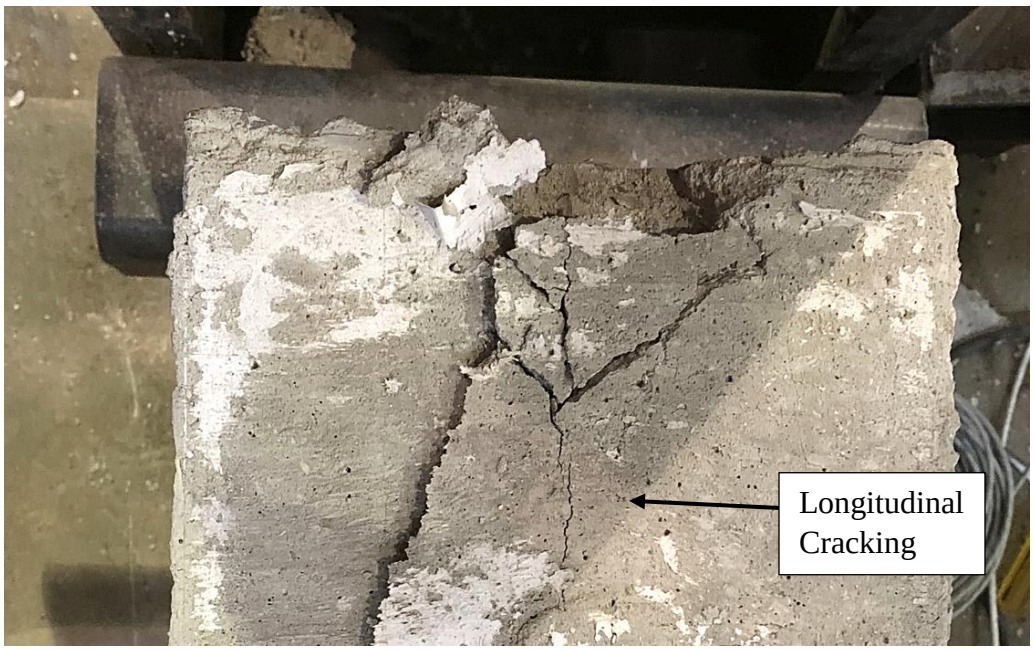

Figure 35: Top of Control Specimen #1 after failure.

Figure 36: Longitudinal cracking along bonded length of Control Specimen #1.

Figure 37 shows Control Specimen #1's bonded length, after it failed. While it is difficult to see in the photograph, the bearing surface (where the reinforcing bar lugs bond to the concrete) on the side of the bar that was pulled in tension are crushed, while the back side is not. This is commonly seen in bond tests as the concrete crushes in the regions adjacent to the bearing surfaces of the reinforcing bar.

Figure 37: Close-up of bonded length of Control Specimen #1 after failure.

The resulting bond load vs. slip curves measured from the fix-end and free-end are seen in Figure 38 and Figure 39 respectively. This specimen had a maximum bond load of 6551-lbs with a fixed-end bond slip of 0.0159" and a free-end bond slip of 0.00472" (Table 9). These graphs illustrate the sudden and brittle failure experienced by this specimen as there is no residual strength after the ultimate load is reached. Interestingly, the free end slip increased significantly (from about 0.0015 in. to 0.0047 in.) in the 20 seconds before failure and last 100 lbs of loading. This is likely due to the longitudinal crack in Figure 36 being formed and allowing the bar to slip.

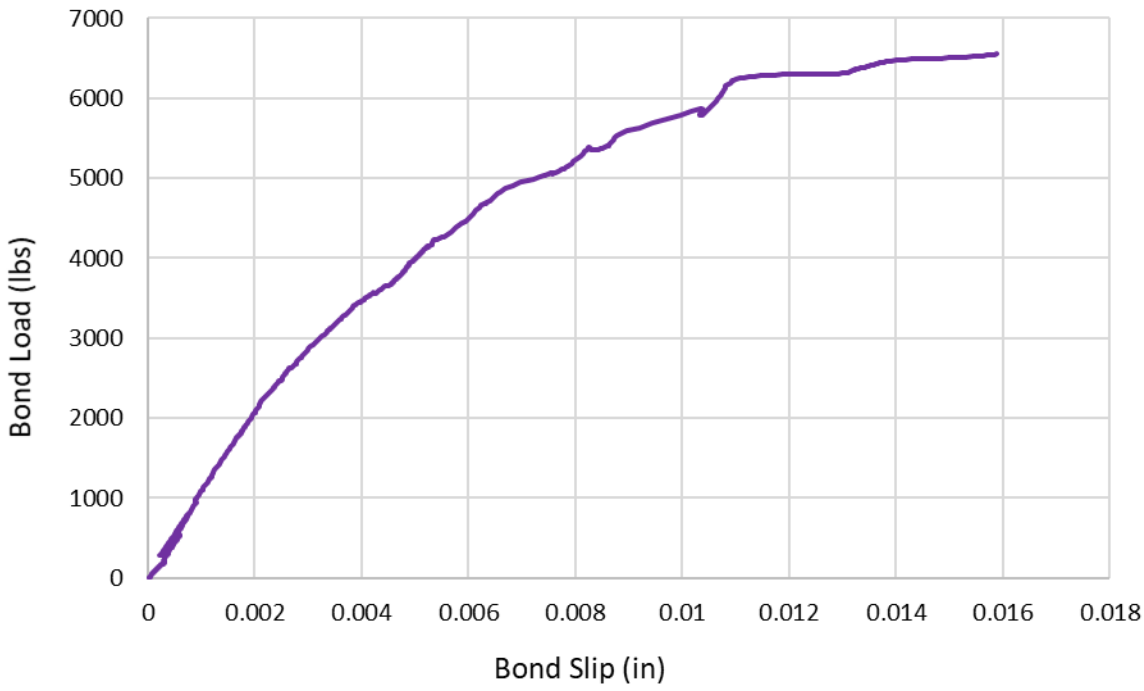

Figure 38: Fixed-end bond load vs. bond slip for Control Specimen #1.

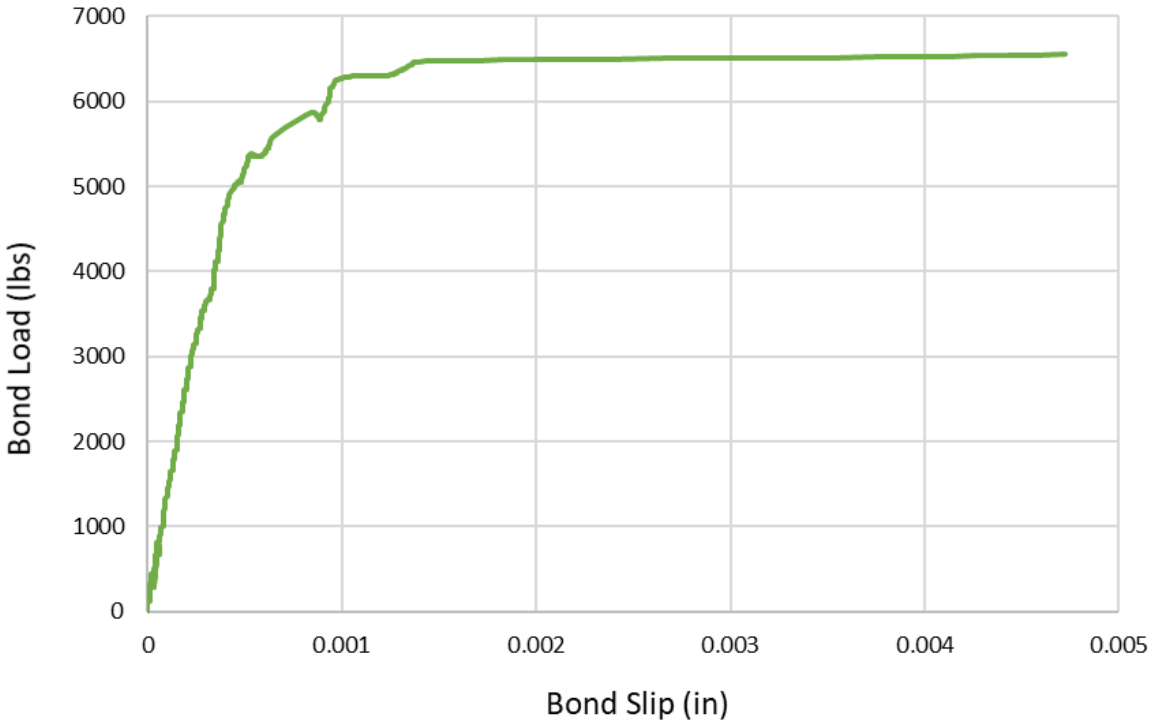

Figure 39: Free-end bond load vs. bond slip for Control Specimen #1.

4.1.2 Control Specimen #2

Similar to the first control specimen, Control Specimen #2 (Figure 40) is monotonically loaded until failure. This specimen has an actual bonded length of 4.875" and a cover depth of 0.464" (Table 7).

Table 7: Properties of Control Specimen #2

Actual Bonded Length, l_d (in.)	Actual Cover Depth, c_d (in.)
4.875	0.464"

Figure 40: Control Specimen #2 prior to testing.

Figure 41 shows a top view of Control Specimen #2 after it failed.

Figure 41: Top-view of failure surface of Control Specimen #2.

Figure 42 shows a close-up, front view of the failed beam. This specimen, much like the first one, experienced a splitting failure as the bond stress capacity was reached. One main difference in this specimen's failure method is a lack on longitudinal cracking occurring over the length of the reinforcing bar. This specimen had a much more abrupt failure than Control Specimen #1 due to no longitudinal cracking (which reduced confining pressure gradually).

Figure 42: Front-view of failure surface of Control Specimen #2.

Again, while it is difficult to see in the photo, this specimen also experienced concrete crushing on the bearing side of the lug. The opposite side of the lug showed no sign of crushed concrete (Figure 43).

Figure 43: Close-up of bonded length of Control Specimen #2 after failure.

The bond load vs. slip curves measured for Control Specimen #2 from the fix-end and free-end are seen in Figure 44 and Figure 45 respectively. This specimen had a maximum bond load of 6478-lbs with a fixed-end bond slip of 0.014” and a free-end bond slip of 0.0011”. The free end slip (0.0011 in.) is much less than that of Control specimen

#1(0.0047 in.). This is likely due to the absence of the longitudinal crack and the failure of the bond caused by the splitting of the concrete cone.

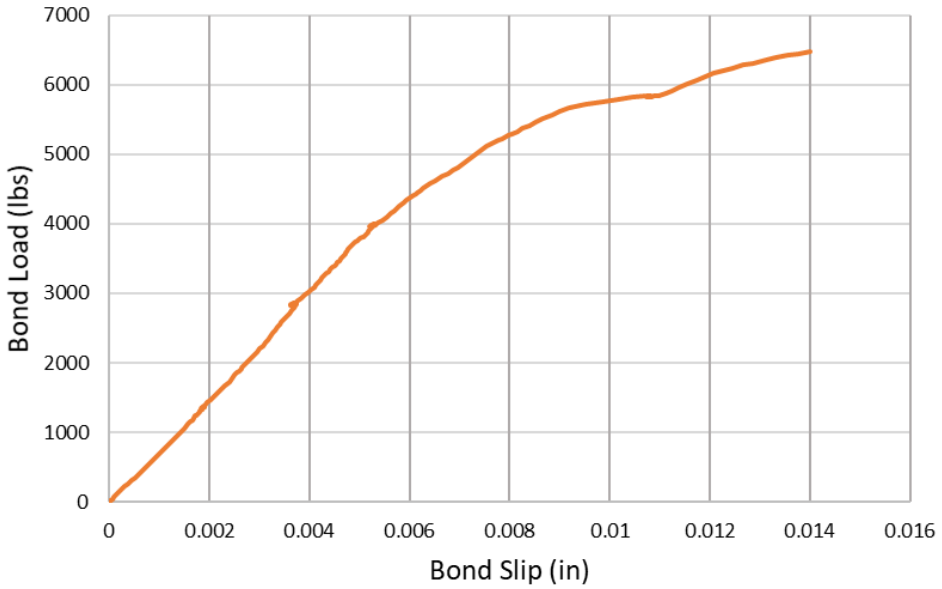

Figure 44: Fixed-end bond load vs. bond slip for Control Specimen #2.

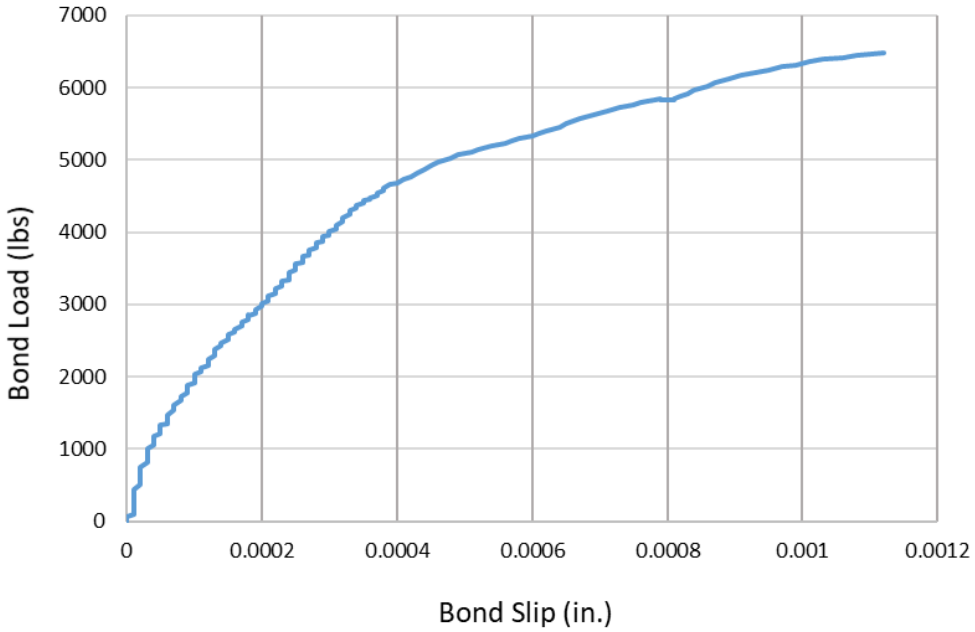

Figure 45: Free-end bond load vs. bond slip for Control Specimen #2.

4.1.3 Control Specimen #3

Similar to the first two control specimens, Control Specimen #3 (Figure 40) is monotonically loaded until failure. This specimen has an actual bonded length of 4.98" and a cover depth of 0.429" (Table 8).

Table 8: Properties of Control Specimen #3

Actual Bonded Length, l_d (in.)	Actual Cover Depth, c_d (in.)
4.98"	0.429"

Control Specimen #3 had a fairly similar failure (large longitudinal cracking) as experienced by Control Specimen #1. This longitudinal cracking, seen in Figure 46 and Figure 47, weakens the confining pressure on the bar causing it to pullout.

Figure 46: Front end of failed Control Specimen #3.

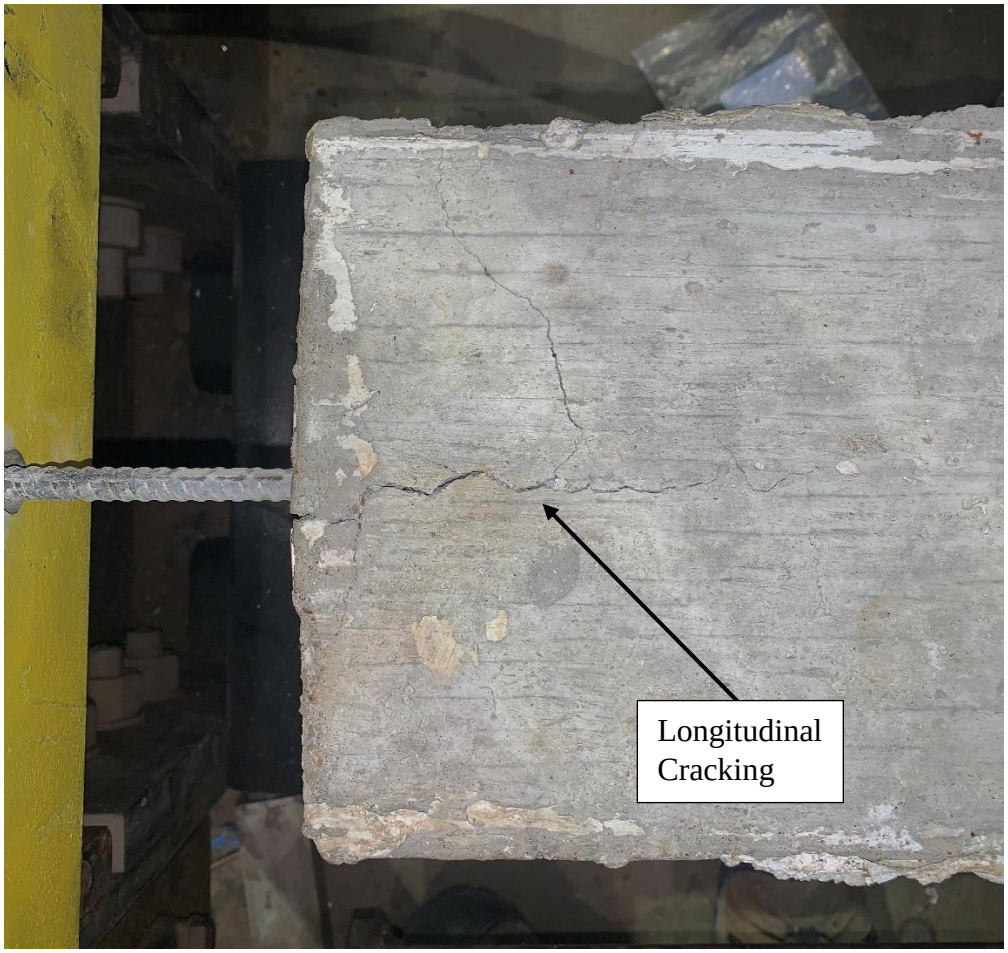

Figure 47: Top-view of failed Control Specimen #3.

The resulting bond load vs. slip curves measured from the fix-end and free-end are seen in Figure 48 and Figure 49 respectively. This specimen had a maximum bond load of 6676-lbs with a maximum fixed-end bond slip of 0.0212” and a maximum free-end bond slip of 0.00224” (Table 9). This specimen also experienced sudden, brittle failure with no residual strength after the ultimate load is reached. The free-end of the reinforcing bar behaved similarly to Control Specimen #1 near the end of loading. The free-end slip increased from about 0.00165” to 0.00215” in the 20 seconds before failure and last 110 lbs of loading. This is likely due to the longitudinal crack, shown in Figure 46, being formed and allowing the bar to slip.

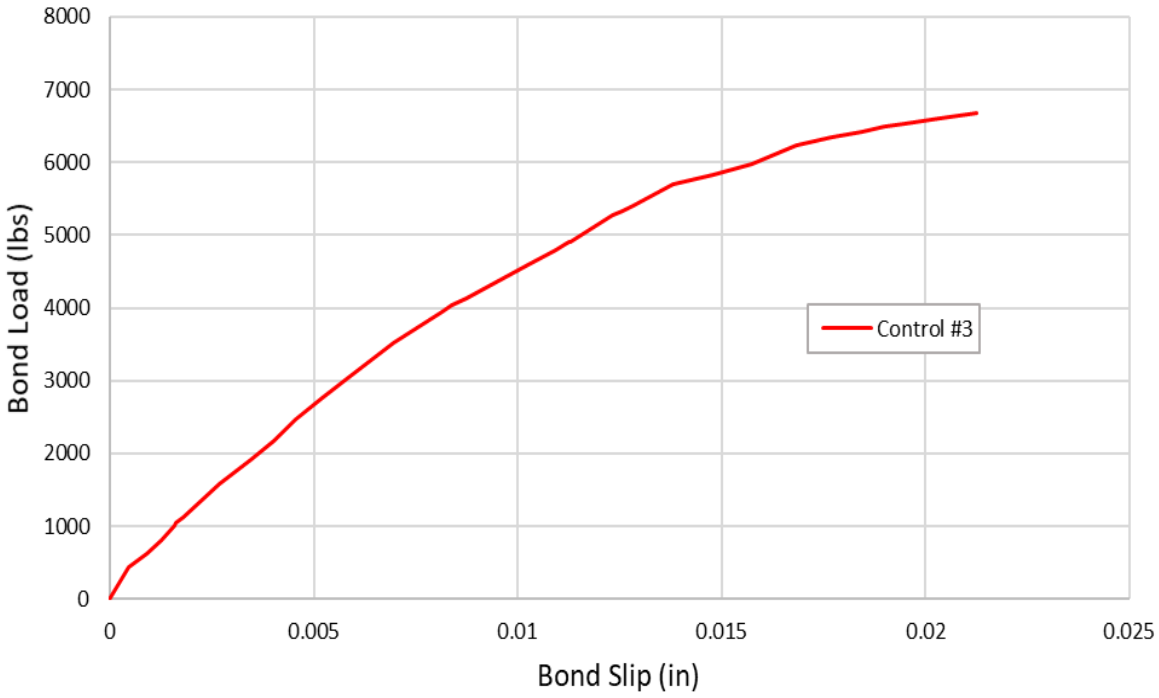

Figure 48: Fixed-end bond load vs. bond slip for Control Specimen #3.

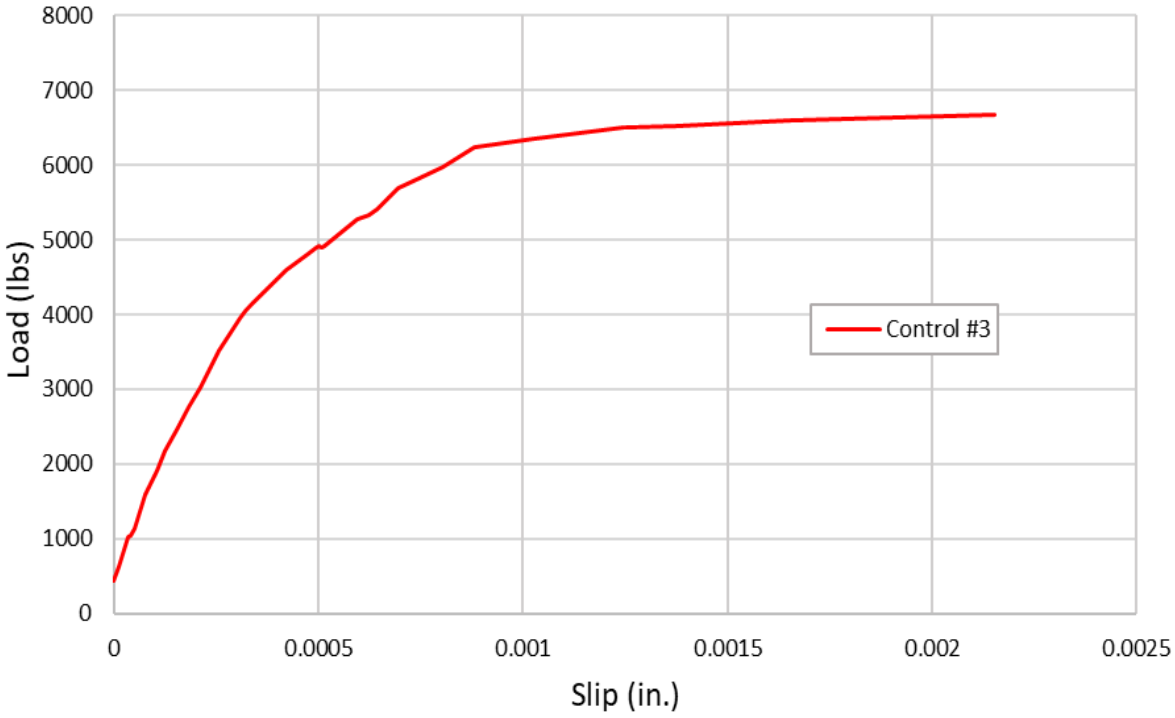

Figure 49: Free-end bond load vs. bond slip for Control Specimen #3.

4.1.4 Overall Control Specimen Results

Table 9 gives the results of the 3 control tests. Control Specimen #1 had an ultimate bond load capacity of 6551-lbs, which is only 1.11% higher than Control Specimen #2 and 1.9% lower than Control Specimen #3. The fixed-end slip at failure is 11.9% higher for #1 when compared to #2 and 25% higher when compared to #3. The largest difference was the maximum free-end slip; Control Specimen #1 slip was 76% higher than Control #2 and 52% higher than Control #3. This difference was likely due to the longitudinal crack that allowed additional slipping before failure in Control Specimen #1. Control Specimen #3 also had longitudinal cracking, which lead to more free-end slip than Control #2, but not as much as Control #1. Overall, the fairly consistent load and fixed end slip indicates uniformity among the specimens and a good basis for the control strength. The average ultimate bond load for the control specimens was 6568 psi; this will be used to determine loading percentages for the sustained tests.

Table 9: Results of Control Specimens

	Maximum Fixed-end Slip	Maximum Free-end Slip	Ultimate Bond Load
Control Specimen #1	0.0159”	0.00472”	6551 lbs.
Control Specimen #2	0.014”	0.0011”	6478 lbs.
Control Specimen #3	0.0212”	0.00224”	6676 lbs.

4.1.5 Expected Control Test Results

ACI Committee 408, the committee for "Bond and Development of Straight Reinforcing Bars in Tension', states that the test results for bond specimen exhibit large scatter in data. The scatter actually increases as test results from different laboratories are compared. The reason for this large scatter in data is a result of differences in concrete properties as concrete is an inherently variable material. Main factors that affect the bond test results are fracture energy and reinforcing bar geometry – factors not usually considered in reinforced concrete design. While this large scatter of data makes it difficult to narrow down expected results in any one given bond test, ACI Committee 408 gives refined equations for calculating bond strength that depend on bond length, cover depth, area of the reinforcing bar, and the strength of the concrete.

The process of calculating the expected bond force at failure is determined by

$$T_b = T_c + T_s \tag{4.1}$$

where T_b is the total bond force developed, and T_c and T_s are the components of this bond force caused by concrete and transverse steel respectively. Because the beam-end specimens used in these tests are without transverse steel in the bond area, it is assumed that T_s = 0. Therefore, the total bond force developed is $T_b = T_c$.

The ACI Committee 408 gives the following equation to calculate the bond force:

$$\frac{T_c}{{f'_c}^{1/4}} = [59.9 l_d (c_{min} + 0.5 d_b) + 2400 A_b] \left(0.1 \frac{c_{max}}{c_{min}} + 0.9\right) \tag{4.2}$$

where l_d is the bonded length, c_{min} is the cover depth, d_b is the diameter of the reinforcing bar, A_b is the area of the reinforcing bar, and c_{max} is the maximum cover

depth. For a beam-end bond test, there is only one reinforcing bar developing bond force, so there is only one *c* value, so equation (4.2) reduces to

$$T_c = [59.9 l_d (c_d + 0.5 d_b) + 2400 A_b] * {f'_c}^{1/4} \quad (4.3)$$

Using this value for the bond force, T_c, the expected bond stress can be calculated (Table 10).

$$u_{exp} = \frac{T_c}{\pi d_b l_d} \quad (4.4)$$

Table 10: Expected and actual results of bond force and bond stress.

	ACI Approach		**Measured**	
	Expected Bond Force, $T_{c,exp}$ (lbs.)	Expected Bond Stress, u_{exp} (psi)	Actual Bond Force, T_c (lbs.)	Actual Bond Stress, u (psi)
Control Specimen #1	3812	655	6551	1126
Control Specimen #2	3929	675	6478	1113
Average	-	-	6514.5	1119.5

Using the ACI 408 method of calculating the expected bond forces showed conservatism in the ACI 408 method. The actual bond force and stress for Control Specimen #1 was

about 71.8% higher than ACI. The bond force and stress for Control Specimen #2 was 64.8% higher.

As these tests are scaled down (3/8” aggregate and #3- reinforcing bar) no previous results of beam-end specimens at this size could be found. Bond relies heavily on the outer perimeter of the reinforcing bar to determine the strength (larger bars have more area for concrete to bond to and thus have larger bond strength). While the overall load and slip cannot be compared directly, the shape of the curve can. Figure 50 shows previous results of beam-end bond test preformed to compare the effect that using different cement types has on bond strength. The loads and slippages are noticeably higher (as expected as these are #6 bars being tested); the shape of the curve does line up with the curves in our control beam-end bond tests.

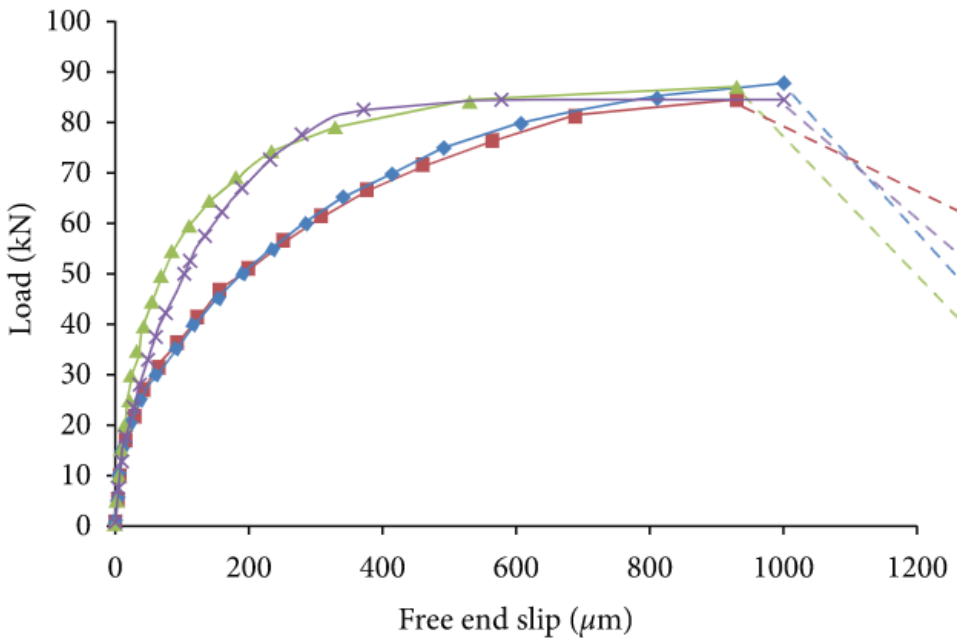

Figure 50: Free-end slip of different cement types [Cui,2020]

4.2 Sustained Loading Results

4.2.1 Sustained Specimen #1

For the first sustained load test, the bond specimen was loaded to 5285-lbs which was 81.1% of the expected ultimate strength found from the control specimen's capacities. This load was maintained a duration of 30 days. After 30 days, the load was gradually increased by steps of about 100 to 200-lbs every 2-3 days. This process of increasing the load happened over a length of 28 days until the specimen reached a bond load of 7327-lbs and failed.

Table 11: Properties of Sustained Specimen #1.

Actual Bonded Length, l_d (in.)	Actual Cover Depth, c_d (in.)
5.25	0.4375

Figure 51: Sustained Specimen #1 prior to testing.

Figure 52 shows the fixed-end of Sustained Specimen #1 after it failed minutes after the load was increased to 7327-lbs. This specimen exhibited a splitting failure just as both control specimen did. No longitudinal crack prior to failure was noticed.

Figure 52: Fixed-end of Sustained Specimen #1 after failure.

The bearing surface on the reaction side of the lugs for Sustained Specimen #1 had visibly more concrete crushed than the control specimens. This increase of crushed concrete shows the increased slippage of the reinforcing bar at the concrete interface.

Figure 53: Close-up of bonded length of Sustained Specimen #1 after failure.

The high-sustained loading applied did not result in failure of this specimen; it failed shortly after the load was increased to 7327-lbs. Although it did not fail under sustained

loading, the effect that sustain loading had on the slip behavior is apparent when it is compared to the control specimens. Additionally, the load at failure was 11.5% higher than the control specimens. The higher load seems to indicate that under high sustained load the plastic deformation of the cement paste allowed for more load to be carried. Additional tests will help to verify this.

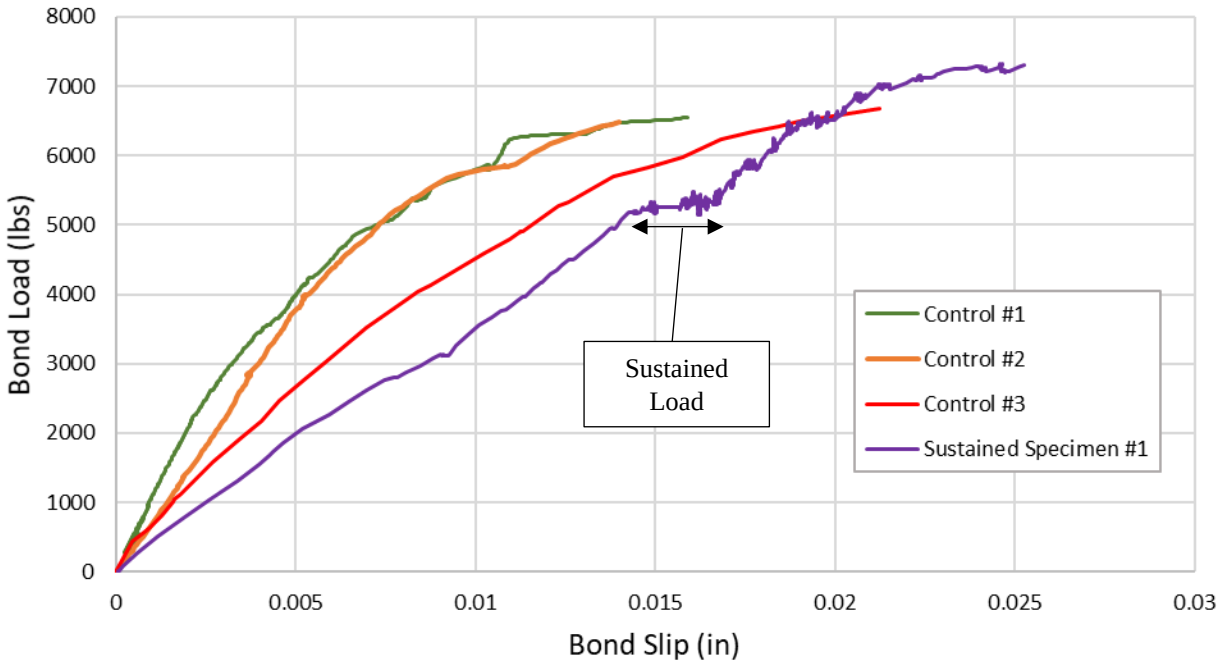

Figure 54: Fixed-end bond load vs. bond slip for Sustained Specimen #1

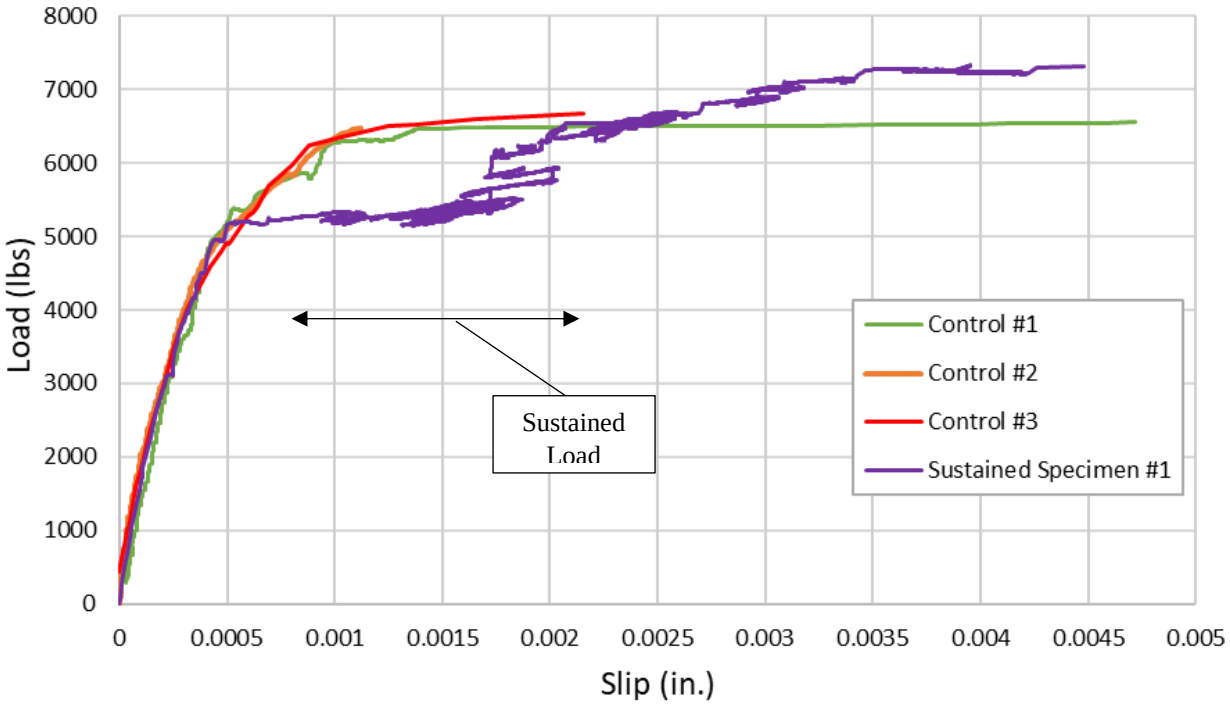

Figure 55: Free-end bond load vs. bond slip for Sustained Specimen #1.

Figure 54 shows the fixed-end bond slip with respect to the bond load. Figure 55 shows free-end bond slip with respect to the bond load. The regions of sustained loading are indicated in the figures. Both figures show increased slip during the sustained load.

The maximum fixed-end slip was 0.0252-inches which is 59% larger than the average of the three control specimens. However, the initial curve of the fixed-end did not match up with the control curves; it had a lower stiffness compared to the control specimens.

The maximum free-end slip, seen in Figure 56, was 0.00448-in which is 5.1% smaller than Control #1, 75.4% larger than Control #2, and 50.9% larger than Control #3. The free-end values of the control specimens were different due to different failures.

However, the lack of a longitudinal crack in the sustained load specimen would lend comparison to Control Specimen #2.

The slip vs. time curve, shown below in Figure 56, is another good visualization of the increase of slip with time. The sustained load for Specimen #1 lasted to about 700-hours. After this the load was gradually increased by steps of about 100 to 200-lbs every 2-3 days. The shape of the slip vs. time curve, prior to the increase in load, matches the expected shape from concrete creep and beam tests. During this time period of sustained loading, the free-end deflection increases from about 0.0006” to 0.0016”; this is a 62.5% increase in slip – without increasing the load. The fixed-end slip (Figure 57) had a similar curve shape as the free-end. Under nearly constant load (Figure 58), the fixed-end slip increased from 0.0144” to 0.0169”; this is an increase in slip of 17.4%.

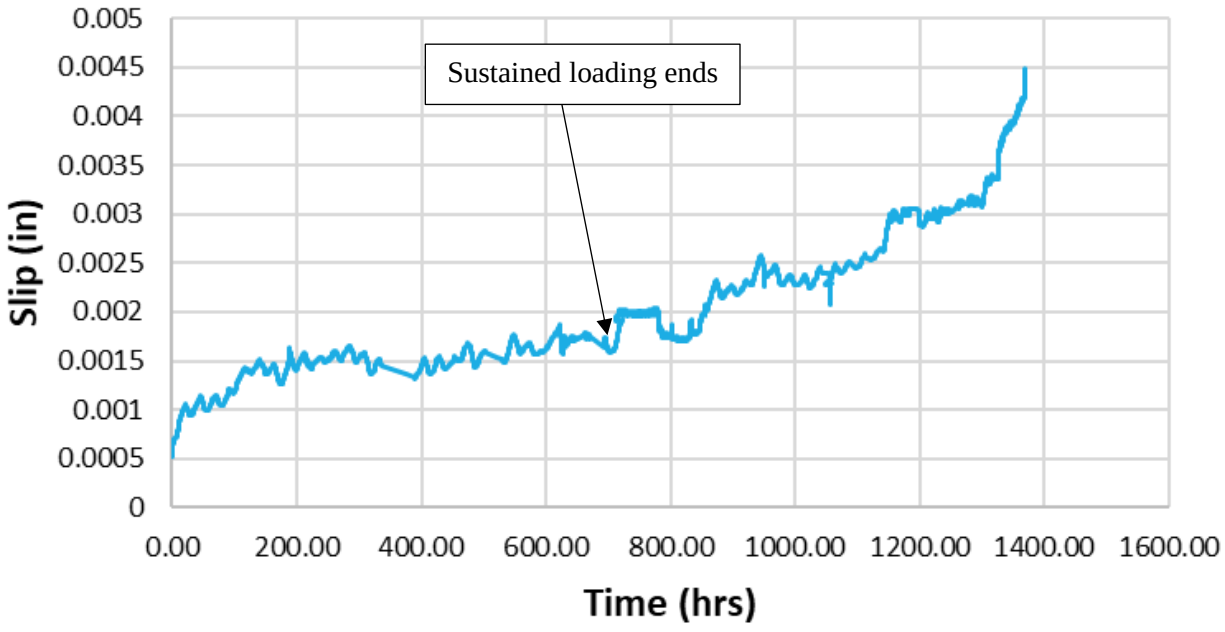

Figure 56: Sustained Specimen #1 free-end slip vs. time.

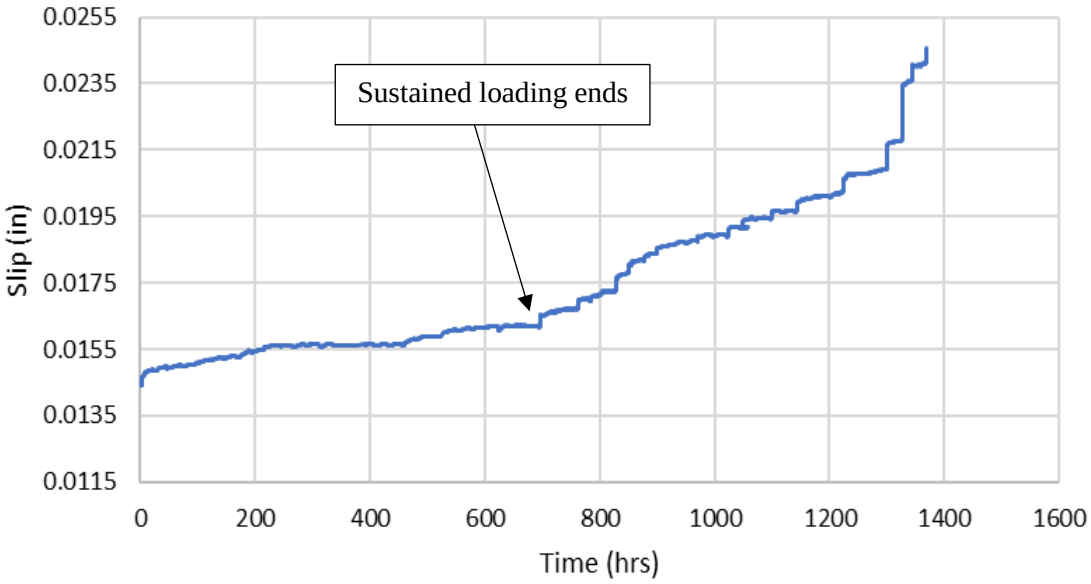

Figure 57: Sustained Specimen #1 fixed-end slip vs. time.

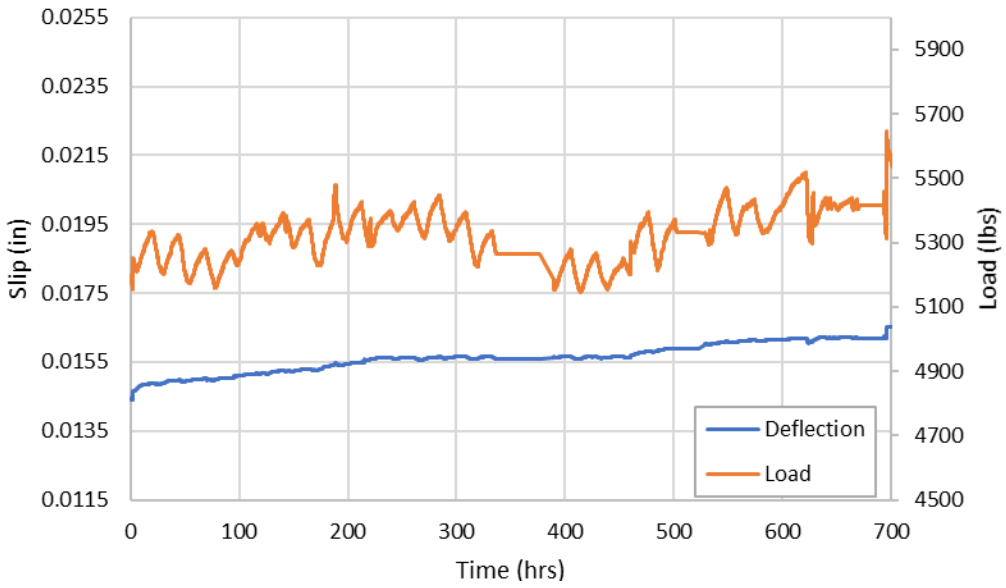

Figure 58: Sustained Specimen #1 slip vs. time plotted with load with time.

4.2.2 Sustained Specimen #2

The second sustained test was loaded to 5850-lbs, which is 89.8% of the expected ultimate strength of the control specimens. This test has not experienced failure yet, but the load has been held for a duration of about 22 days.

Figure 59: Sustained Specimen #2 ready to be loaded.

For Sustained Specimen #2, both the fixed-end and the free-end initial bond slip responses matched closely with the control tests; these results can be seen in Figure 60 and Figure 61 respectively. The specimen was loaded to about 90% of the expected ultimate strength where it then experienced an increase in deflection with a constant

applied load. The regions of sustained loading are indicated in the figures. Both figures show increased slip during the sustained load.

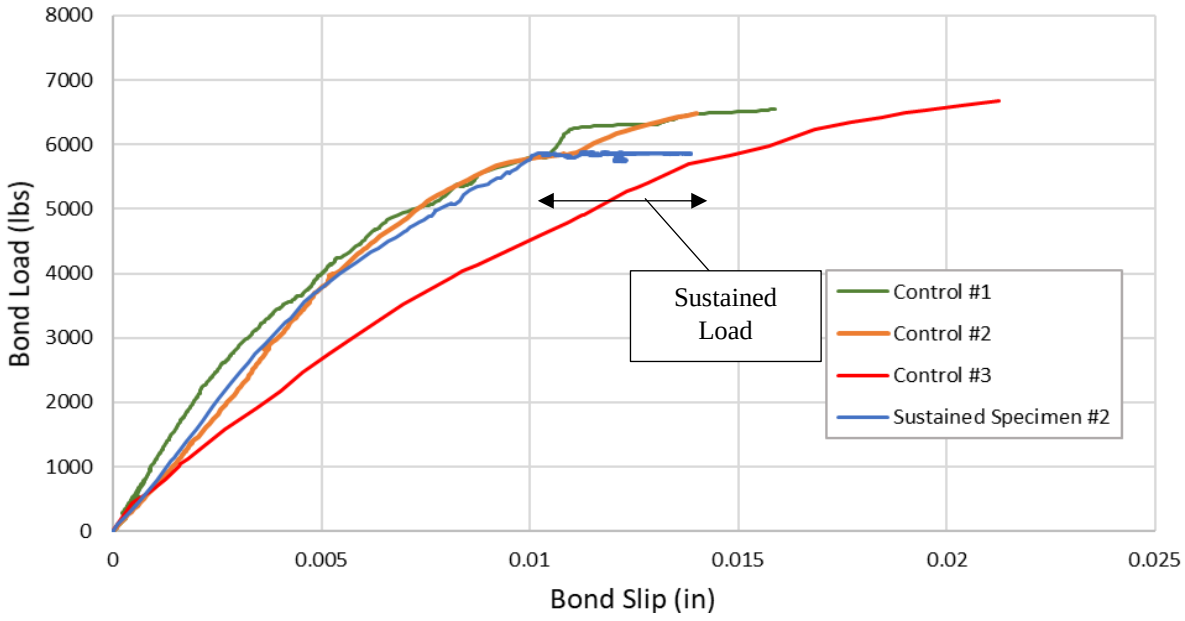

Figure 60: Fixed-end bond load vs. bond slip for Sustained Specimen #2.

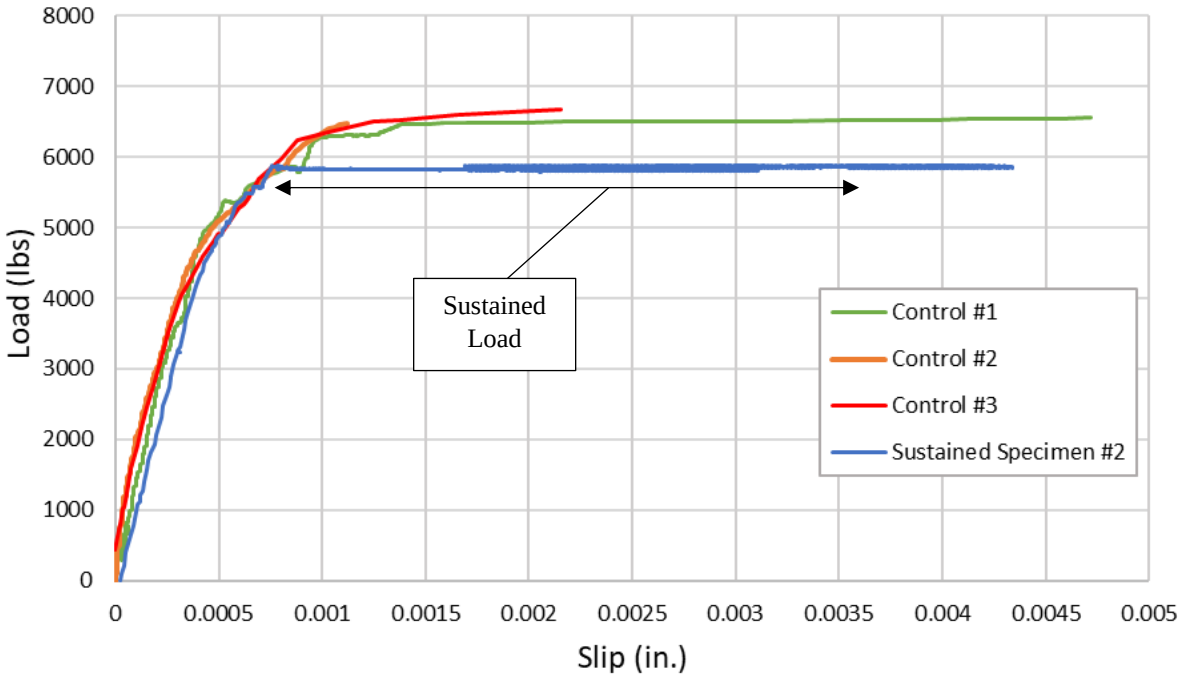

Figure 61: Free-end bond load vs. bond slip for Sustained Specimen #2.

Figure 62 shows that free-end slip with time under sustained loadings. During this time period, the slip increased from 0.00076” to 0.0033”. This is 0.00254” or a 334% increase in slip. There are large amounts of fluctuations in this free end data; part of this is due to this LVDT measuring very small deflections, so slight thermal contractions and expansions are prevalent. The overall shape of the logarithmic trendline does match with what was seen in the first sustained test as well as concrete creep theory.

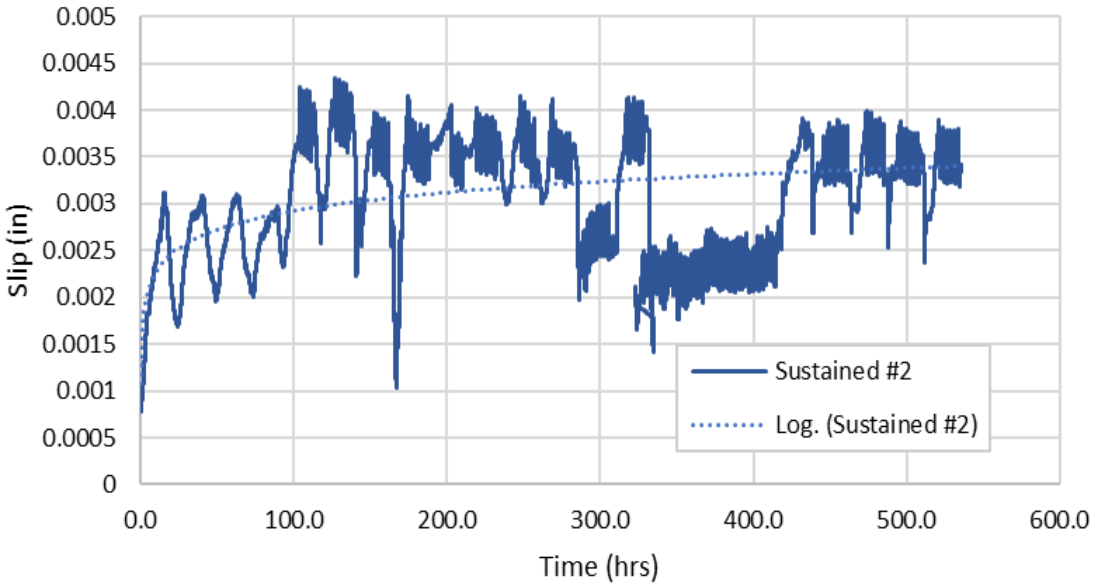

Figure 62: Sustained Specimen #2 free-end slip vs. time curve.

The fixed-end slip reading increased from 0.0103” to about 0.0121” under sustained loading; this is an increase of 17.4%. The fixed-end LVDT is noticeable less sensitive to temperature fluctuations because it is measuring larger displacement values compared to the free-end LVDT. Regardless of oscillations caused by temperature, both the fixed and free-ends experienced substantial deflections under high sustained load (with similar looking trendlines).

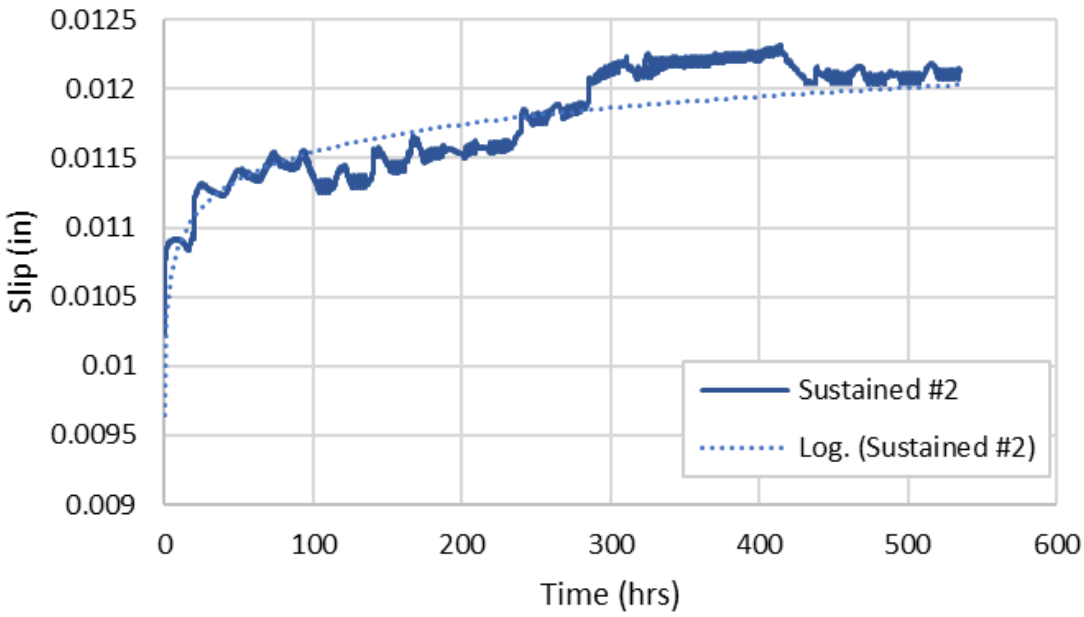

Figure 63: Sustained Specimen #2 fixed-end slip vs. time curve.

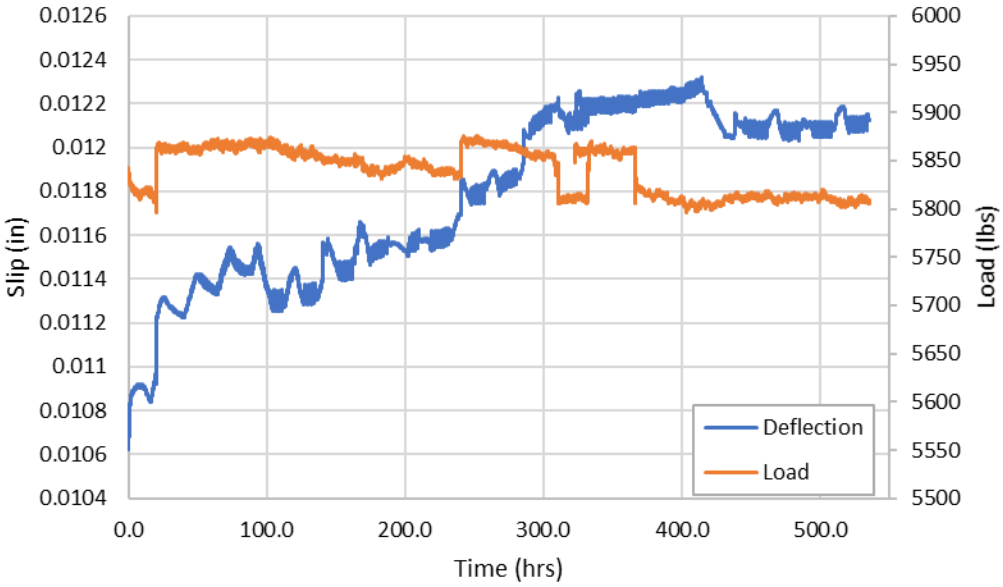

Figure 64: Sustained Specimen #2 fixed-end slip vs. time curve with load.

4.2.3 Sustained Specimen #3

The expected ultimate strength for these bond specimens will change as more and more specimens are tested (leading to a better estimate of the expected ultimate strength). Sustained Specimen #3 is the first sustained specimen that is affected by this refining process. The ultimate strength of Sustained Specimen #1 was 12% higher than the expected ultimate strength from the control specimens; thus, the average of the ultimate strengths of all tested specimen increases. Sustained Specimen #3 is loaded to 6550-lbs which is 96.4% of the average ultimate strengths of all the specimen; if sustained loading does increase the capacity of the specimens, it is loaded to 88.1% of the sustained capacity (based purely on Sustained Specimen #1's ultimate strength).

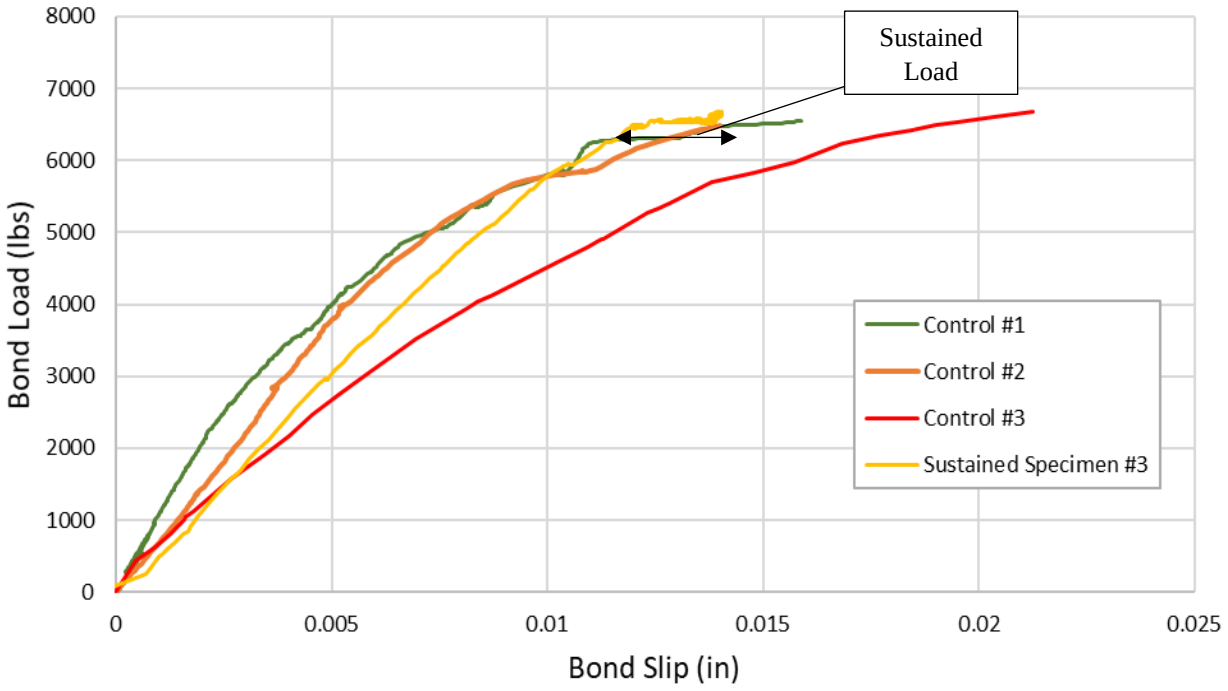

Figure 65: Sustained Specimen #3 fixed-end bond load vs. bond slip.

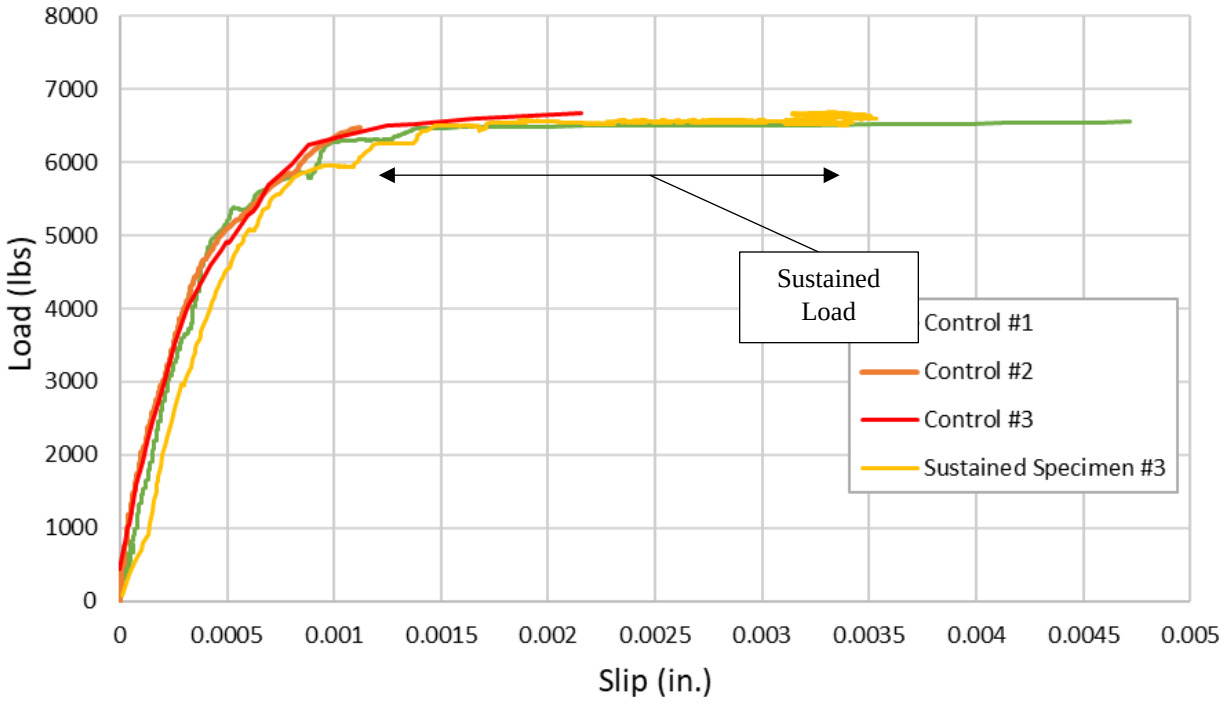

Figure 66: Sustained Specimen #3 free-end bond load vs. slip.

The shape of free-end slip vs. time curve, seen in Figure 67, matches closely with the curves seen in expected concrete creep and in the sustained beam test. This specimen, loaded past the expected threshold of 0.8f'c, has not yet reached tertiary creep, but the test is ongoing.

Figure 67 shows the slip of the reinforcing bar under sustained load. After 220 hours of loading, the increased from 0.00173" to 0.00346". This is an increase in slip of exactly 100%, meaning that under sustained loading, the rebar deflection (measured from the free-end) doubled. Slip at a time of 220 hours for Specimen #1 increased from 0.00072" to 0.00146"; this is a 50.7% increase in slip. Slip for Specimen #2 in 220 hours increased from 0.00076" to 0.00346", a 78% increase in slip. This means that Sustained Specimen #3, loaded 1265-lbs higher than Sustained Specimen #1 has 49.3% more deflection in this time period. Specimen #3 is loaded 700-lbs higher than Specimen #2 and has 22% more

deflection under sustained load. This data follows the trend of increased bond slip under higher sustained loading.

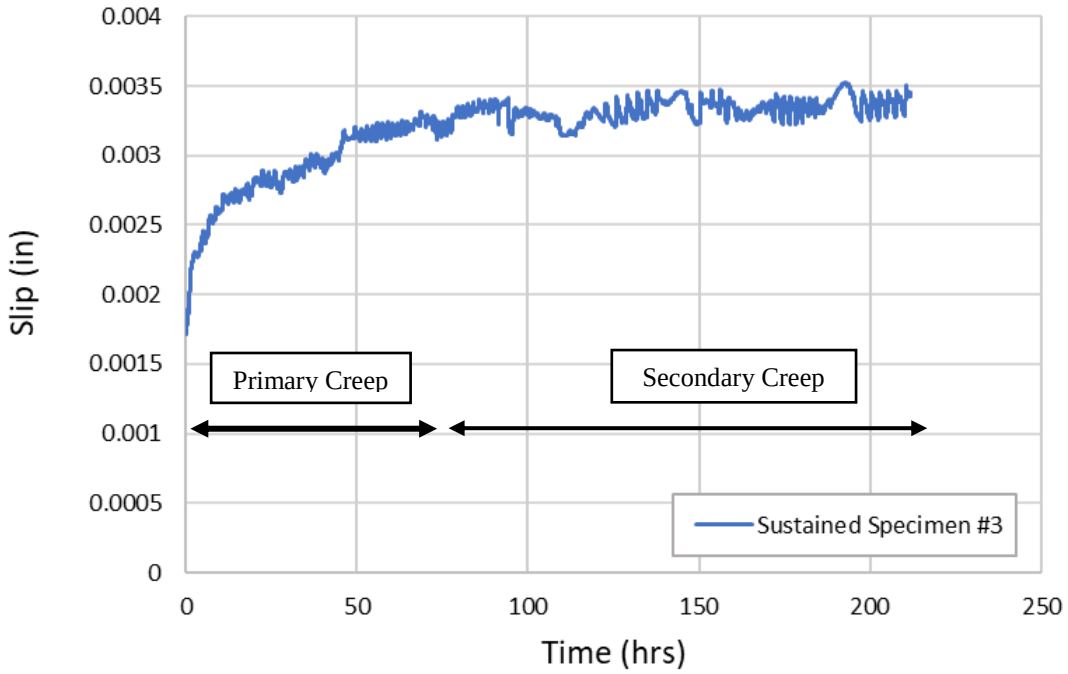

Figure 67: Time vs. free-end slip for sustained portion of loading for Sustained Specimen #3.

The sustained test for Specimen #3 began on November 20th. The lab in the winter months is heated which reduced fluctuations due to temperature. The result of this is smoother data obtained from both LVDT's as the temperature effect is minimized. Both Figure 67 and Figure 68 show the slight cyclical behavior of heating the lab. This data is much smoother than Sustained Specimen #1 and #2 which were tested without climate control and thus experienced larger temperature swings.

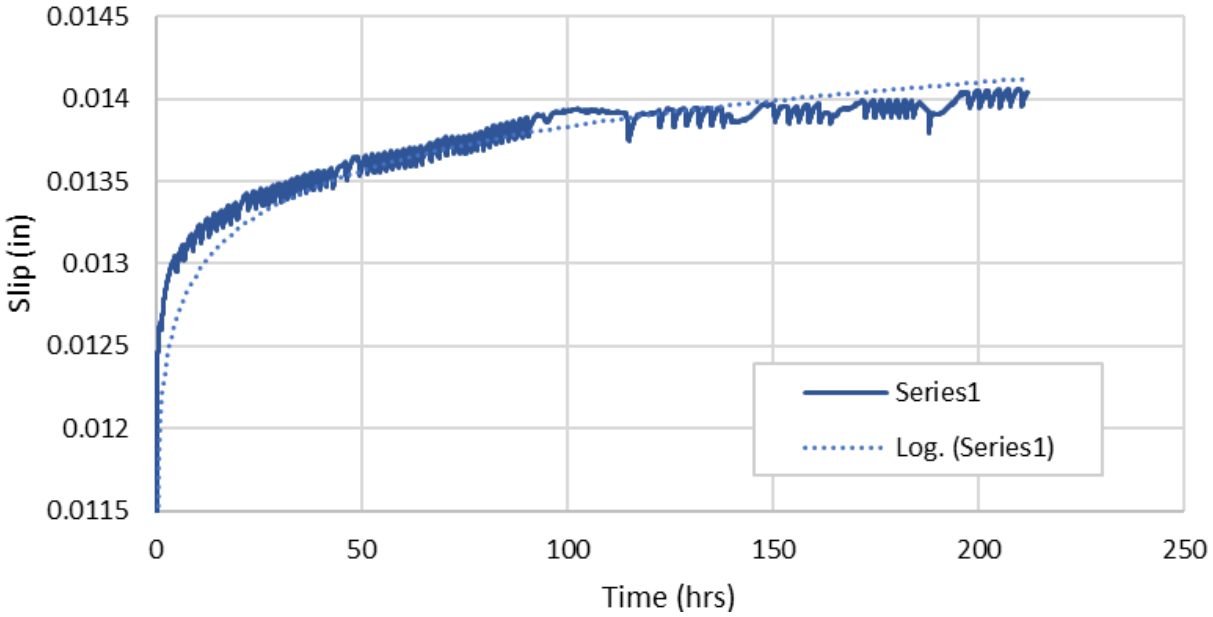

Figure 68: Time vs. fixed-end slip for sustained portion of loading for Sustained Specimen #3.

4.3 Temperature and Humidity Effect

The jagged behavior of the sustained loaded portions of all the graphs in Section 4.2 are a result of a fluctuation in temperature and humidity at the testing location. While temperature and humidity were unable to be controlled, they were monitored at the same time as the other data being recorded. By overlapping the temperature and humidity data on the Slip vs. Time curves (Figure 69) trends in the data can be seen.

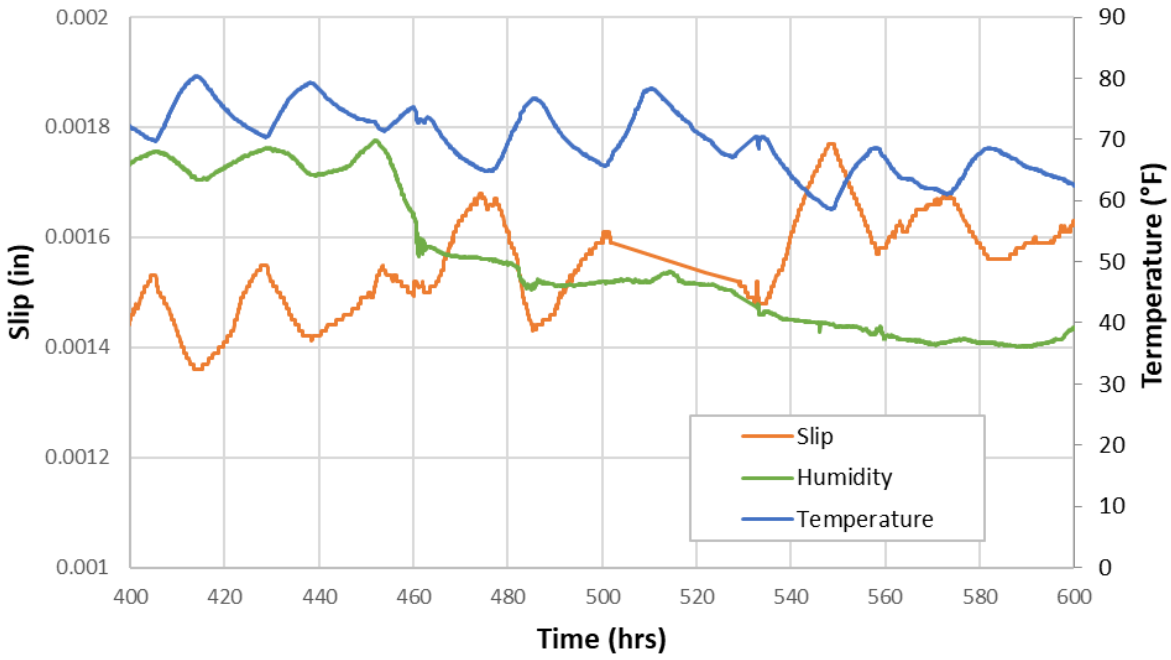

Figure 69: Typical temperature and humidity effect of slip in sustained bond specimen.

The most apparent relationship gathered from this is the increase in slip that occurs as the temperature drops. Steel, a conductor, is more susceptible to changes in temperature than concrete; in this case there is a large volume of steel outside of the concrete that contracts as the air around it cools off. This contraction results in higher bond force applied to the bar. Typically, a 10°F decrease in temperature results in a 9.75% increase in slip.

Likewise, a 10° increase in temperature results in a 9.75% decrease in slip. While fluctuations in load occurred throughout the tests, the average load remained constant throughout. The temperature effect for Specimen #3 is much less because the lab is climate controlled in the winter months causing less of a day-to-day range in temperature (small fluctuations still occur).

Creep theory says that concrete in more humid environments will creep less than concrete in environments with less humidity. This appears to be the case in these sustained bond tests. While it appears that temperature has a greater day-to-day effect on the slippage of the bar, the general trend of decreasing humidity may have led to greater bar slip. The downward trending humidity line corresponds with the upward trending slip line in Figure 69.

4.4 Overall Results

Table 12 contained the results of all the specimens tested. Sustained Specimen #1 had a total free-end bond slip of 0.0048”; of this, 0.0012” of slip occurred under sustained loading. The maximum fixed-end slip was 0.0252” with 0.002” of that occurring under sustained loading. This specimen did have a 12% higher strength than the control specimens. This strength increase could be a result of it having a slightly longer bonded length at 5.063” (the control specimens had bonded lengths of 4.94”, 4.875”, and 4.98”) or due to the effect of the sustained load.

Table 12: Overall results of all beam-end specimen tested.

	Bonded Length	Cover Depth	Maximum Bond Load	Sustained Bond Load	Maximum Fixed-end Bond Slip	Maximum Free-end Bond Slip
Control Specimen #1	4.940”	0.4095”	6551 lbs.	-	0.0159”	0.00472”
Control Specimen #2	4.875”	0.464”	6478 lbs.	-	0.014”	0.0011”
Control Specimen #3	4.98”	0.429”	6676 lbs.	-	0.0212”	0.00224”
Sustained Specimen #1	5.063”	0.4375”	7327 lbs.	5285 lbs.	0.0252”	0.00448”
Sustained Specimen #2	-	-	5869 lbs.	5850 lbs.	0.0121”	0.00434”
Sustained Specimen #3	-	-	6632 lbs.	6550 lbs.	0.01403”	0.00346”

The shape of the fixed-end curve of Sustained Specimen #1 (tested on Test Setup #1) shows that there may have been a problem with that LVDT’s during the initial load phase; this resulted in less initial stiffness. Sustained Specimen #2 was tested on a Test Setup #2; the fixed-end curve matched very well with both of the first control specimens tested. After the first sustained test was completed on Test Setup #1, the LVDT holder was altered to ensure a tight connection. Sustained Specimen #3 was then tested on test setup #1 and its fixed end curve aligned much better with the other specimens.

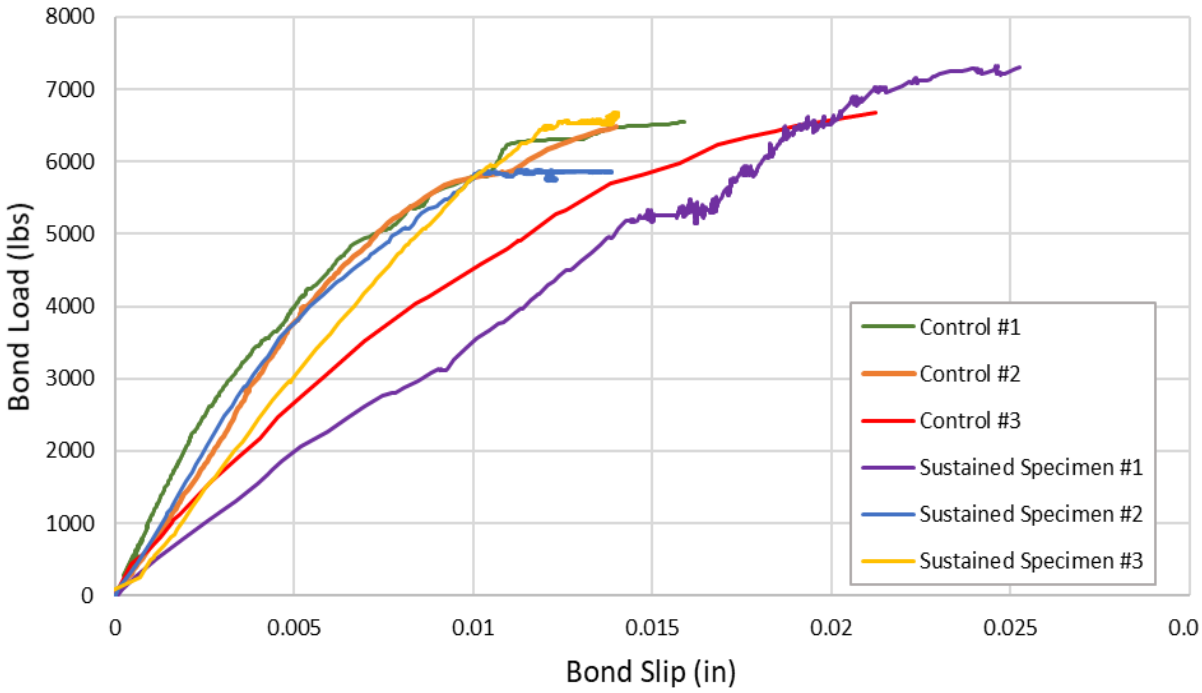

Figure 70: Fixed-end bond load vs. bond slip for all specimens.

Overall, the curves of the free-end slip matched up well with each other. The main difference is seen between the control tests. Control #1 had a large slip prior to failure that wasn't seen in the other control. This large slip is a result of longitudinal cracking occurring along the bonded length which lessens confining pressure and allows greater slip to occur. As the first control test had a cover of only 0.4095", it is hypothesized that this resulted in an inadequate amount of confining pressure to resist longitudinal cracking. Control #2 had a larger cover depth at 0.464" which results in larger confining pressure. This increase in pressure prevented longitudinal cracking and resulted in a more abrupt free-end failure. This abrupt failure caused that specimen to be without a large increase in slip before it failed.

The sustained portions of Figure 71 illustrate how much bond slip occurs under high sustained loading. Sustained Specimen #1 experienced 307% higher slip than Control #2

(compared because of similar failure patterns). Sustained Specimen #2 has 294% higher slip than Control #2 and Sustained Specimen #3 has 214% higher slip thus far.

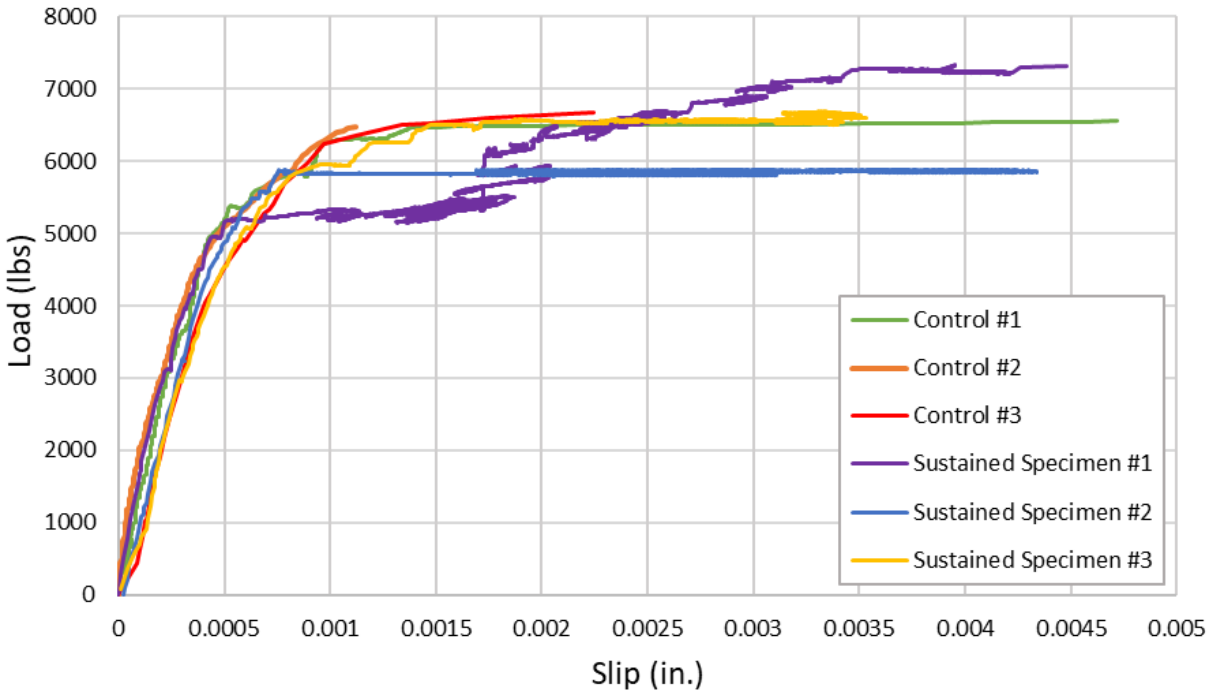

Figure 71: Free-end bond load vs. bond slip for all specimens.

In both the free and the fixed end, there was a constant trend of reinforcing bar slip under sustained load. While the amount of slip varied somewhat, the overall shape of sustained deflection matched expected shapes of creep theory. Unfortunately, due to testing delays, we do not have a large sample of tests to draw conclusions from. However, the trends in data do suggest that bond slip could explain excessive deflection in RC members under high sustained load. Sustained Specimen #1, the only one completely tested, seemed to experience an increase in strength due to sustained loading (12% higher ultimate bond strength). More testing is needed to verify these conclusions.

CHAPTER V BOND SLIP IN FLEXURAL MEMBERS

This section uses knowledge gained from the bond tests in order to explain excessive deflection in concrete beams loaded in flexure under high-sustained stresses.

5.1 Proceeding research

The first tests done for the overall research project were simple reinforced concrete beams subjected to four-point bending. These beams showed the tendency to increase in deflection even as the load is held constant. Of the four beams tested, only three are subjected to sustained loading. The control beam (the first beam tested) is subjected to a monotonic increasing load until failure. At the peak stress, the beam experiences a brittle shear failure as sudden crack propagation splits the beam (Figure 72).

Figure 72: Control beam failing in shear.

Using the control beam's peak loading, three other beams are loaded to certain percentages of the predicted ultimate strength and are left for varying durations. One

beam is loaded at 81% of the expected ultimate flexural capacity for 25 days (B-SL-81), one beam is loaded at 86% for 24 days (B-SL-86), and the last beam is loaded at 92% for 42 days (B-SL-92). As seen in Figure 73, subjecting the beams to sustained loading results in greater deflection and a more ductile failure. Deflection at failure for the sustained loaded specimens were 31% (B-SL-81), 44% (B-Sl-86), and 21% (B-SL-92) higher than the control beam.

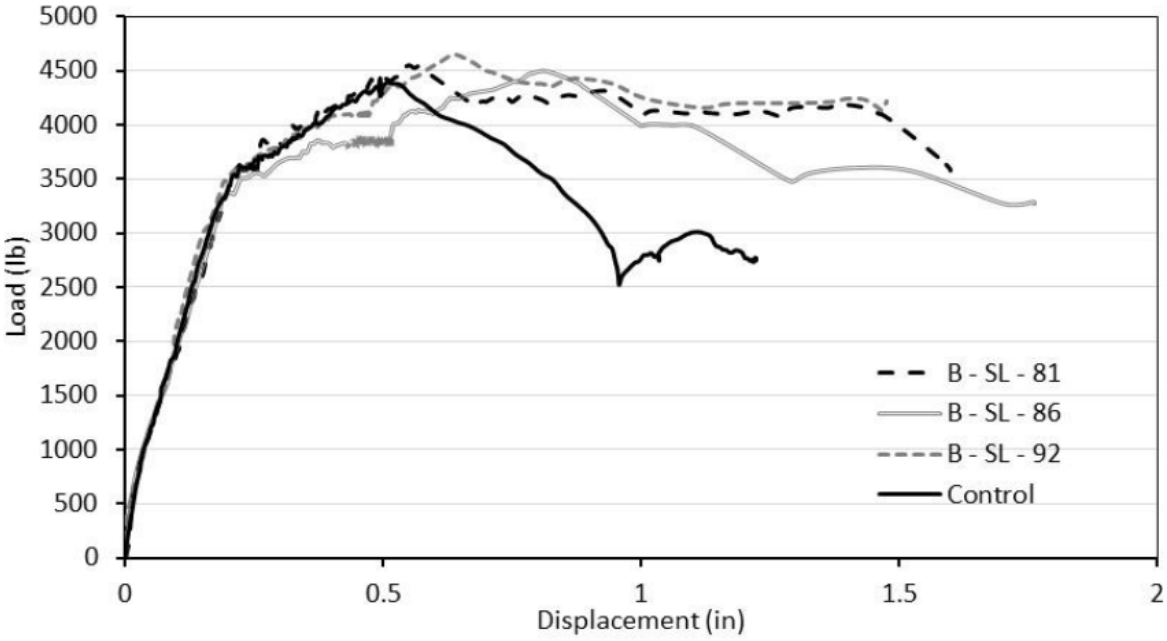

Figure 73: Load vs. deflection response of beams subjected to four-point bending.

During these periods of sustained loading, the beam's deflection increases with time as the load is held constant (Figure 74). While concrete structures in the past have failed under high-sustained loading, these beams did not. Most of the deflection occur at early periods of the loading. In fact, for these beams, an average of 56% of the deflection occurred in the first 7 days of loading. The rate of deflection drops as time increases which indicates that these specimens will likely not experience time-dependent failure.

The beams are then loaded to failure in a time period similar to the control beam. Once the loading resumes, the load deflection curve increases and meets the path of the pre-loaded curve. This behavior continues until the beams experience failure.

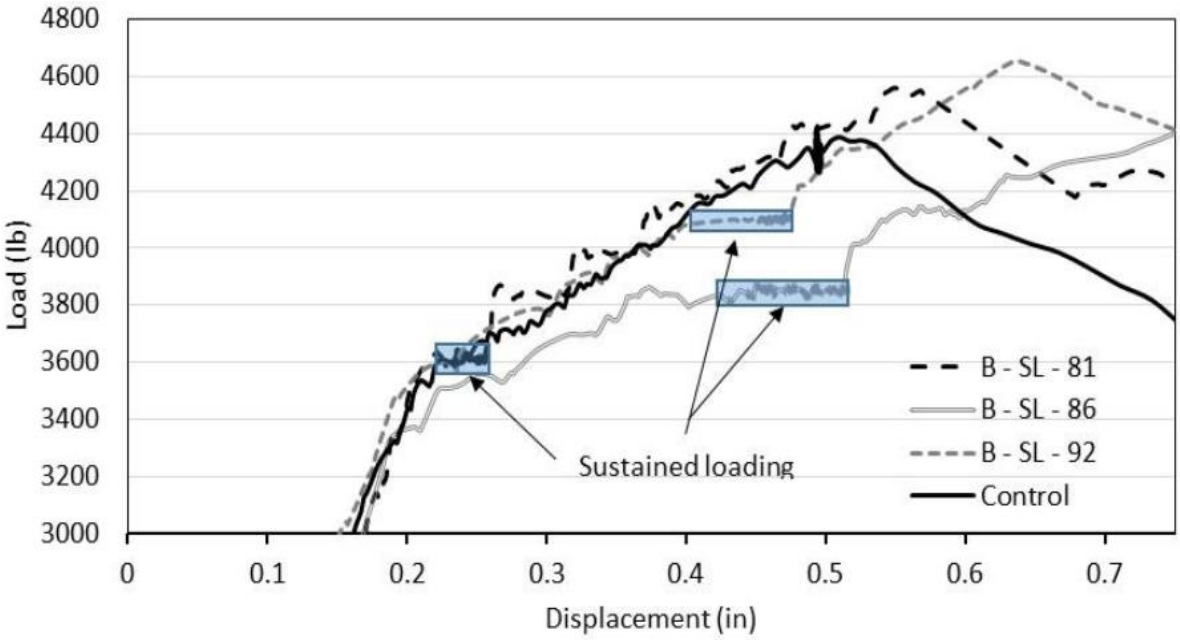

Figure 74: Regions of sustained loading on load vs. deflection graph.

The failures of the sustained loaded beams are much different than the control beam as shown in Figure 75, Figure 76, and Figure 77. One main difference seen in the sustained loaded beams compared to the control beam (Figure 72) is the much larger deflection experienced; on average, there is about a 30% increase in deflection when a sustained load is applied. The other main difference is the large amount of cracking seen in the sustained loaded specimens. This increase in vertical cracking indicates a transition from shear failure (in the control beam) to a more flexural failure (in the sustained beams). This shift in failure modes illustrates how a high sustained load can affect the concrete.

Figure 75: Failure of B-SL-81.

Figure 76: Failure of B-SL-86.

Figure 77: Failure of B-SL-92.

It is hypothesized that a combination of micro-cracking, concrete creep, and slippage of the reinforcement are responsible for the increased flexural response of the beams.

5.2 Initial Deflection

The initial deflection is measured directly from the beam tests by using the deflection data prior to the sustained load. For B-SL-81, the initial deflection is 0.218". The initial deflections of B-SL-86 and B-SL-92 are 0.423" and 0.492" respectively (Table 13).

5.3 Deflection due to Concrete Creep and Bond Slip

Using ACI equations (Appendix) which calculate predicted creep in a concrete member based on the initial loading, the predicted creep deflections are found. These values are given in Table 13. For B-Sl-81, the ACI predicted creep deflection is 0.0372"; the actual measured deflection during the 25-day sustained load period is 0.0403". By subtracting the expected deflection due to creep from the actual deflection measured, the deflection caused by bond slip is found. This value is 0.003" for B-SL-81.

Similar analysis is done for B-SL-86 and B-SL-92. B-SL-86, which was loaded for 41-days, experienced 0.0904-inches of deflection during that time period. 0.0794" of this deflection is the result of concrete creep in the compressive zone; 0.011" of this deflection is the result of bond slip. B-SL-92 was loaded for 24 days. The total sustained load deflection is 0.0838". The sustained load deflection from bond slip is found to be 0.00512". Based off trend in data from the Sustained Bond Tests, the bond slip

experienced under sustained load (free-end) ranges from 0.001” in Sustained Specimen #1 to 0.0018” in Sustained Specimen #3. These numbers are smaller than the expected sustained load deflection caused by bond slip.

Table 13: Deflection measurements for beams under sustained loading.

	Initial Deflection	**Predicted Creep Deflection**	**Actual Deflection during sustained loading**	**Sustained Load Deflection from Bond Slip**
B-SL-81	0.215”	0.0372”	0.0403”	0.003”
B-SL-86	0.4231”	0.0794”	0.0904”	0.011”
B-SL-92	0.454”	0.0786”	0.0838”	0.00512”

These results prove that the slip of the reinforcing bar, caused by high sustained load, results in part of the deflection experienced under sustained load.

VI Summary and Conclusions

6.1 Summary

The present study was carried out in order to find the effect that high sustained loading has on the bond between concrete and No-3 deformed steel reinforcing bars. By using a modified version of ASTM A944 beam-end tests, the bond slip effect under high sustained load is studied directly. Material tests (concrete compression, concrete splitting tension, and steel tension) were also conducted on all materials used in these tests to gain insight on their material properties. All specimens tested for this thesis had design bond lengths of 5" and design cover depths of 0.375". Unfortunately, due to COVID delays, we do not have a large sample of tests to draw conclusions from – only three sustained tests were performed. Nevertheless, trends in data from these tests can still be analyzed.

The control specimens were monotonically loaded until failure in order to determine the ultimate bond strength of the beam-end bond tests. This average bond strength was used as the expected capacity for the sustained bond tests.

Sustained load specimens were tests at sustained load levels of 85 to 90% of the control specimen for a period of at least 3 weeks. Reinforcing bar slip under sustained load was experienced by all the sustained tests. While the amount of slip varied, the overall shape of the sustained deflection matched the expected shapes based on creep theory. The three sustained specimens experienced a range of slip increases of 0.001" – 0.00254" (measured from the free-end) under constant load. The slip under sustained load is 90% to 230% of the slip at failure for Control specimen #2 indicating a significant amount of

slip under sustained load. This suggests that bond slip is one reason for excessive deflection in RC members under high sustained load.

Sustained Specimen #1, the only one tested until failure, experienced a 12% higher bond capacity than the control specimens. While more testing is needed, this rise in capacity may show that bond strength increases due to sustained loading.

6.2 Conclusions

Main conclusions drawn from these tests are as follows:

- There is slip of the reinforcing bar occurring under high sustained load. Sustained Specimen #1 experienced 307% higher slip at failure than Control #2 (compared because of similar failure patterns). Sustained Specimen #2 has experienced 294% higher slip and Sustained Specimen #3 has 214% higher slip thus far.
- The amount of slip increases as the applied load increases. Specimen #1, loaded at 5285-lbs or 81% of the expected capacity, experienced 0.001-inches of slip during 700-hours of sustained loading. Specimen #2, loaded at 5850-lbs or 89.9% of the expected capacity, experienced 0.00254” in just 530 hours. This is a 60.6% increase in slip under sustained load.
- The shapes of the slip vs. time graphs matched what was expected based on concrete creep theory as well as what was seen in previous beam tests as expected.
- Reinforcing bar slip under constant loading likely plays a part in the overall increase in deflection in RC beams tested under high sustained load. The exact extend of this role is yet to be determined.

- Sustained load failure, caused by tertiary creep, was not experienced in these tests.
- Sustained loading may cause an increase in bond strength. Sustained Specimen #1, the only one tested until failure, seemed to experience an increase in strength due to sustained loading (12% higher ultimate bond strength). More testing must be done before definitively concluding that sustained loading increases bond strength.

References Cited

(1) ACI Committee 408. (2003) “Bond and Development of Straight Reinforcing Bars in Tension”, *ACI 408R-03,* American Concrete Institute, Farmington Hills, MS.

(2) Bazant, Zdenek P. and Milan Jirasek. (2018). “*Creep and Hygrothermal Effects in Concrete Structures”*. Springer, pp 1-41.

(3) Bazant, Zdenek P. (1975) “Theory of Creep and Shrinkage in Concrete Structures: A Precis of Recent Developments”, *Mechanics Today,* Vol. 2, pp 1-93, Pergamon Press.

(4) Cox, James V. and Herrmann, Leonard R. (1998). “Development of a Plasticity Bond Model for Steel Reinforcement”, *Mechanics of Cohesive-Frictional Materials,* Vol. 3, pp 155-180.

(5) Goto, Yukimasa, (1971) “Cracks Formed in Concrete Around Deformed Tension Bars”, *ACI Journal,* April 1971, pp 244-251.

(6) Illston, J.M., (1965) “The Creep of Concrete under Uniaxial Tension”, Magazine of Concrete Research, Vol. 17, June 1965, pp 77-83.

(7) Mazumder, Maruful H. (2014) “The Anchorage of Deformed Bars in Reinforced Concrete Members Subjected to Bending”

(8) McCormac, Jack C., Brown, Russell H., (2005) “Design of Reinforced Concrete”, 9E, ACI 318-11 Code Edition.

(9) Rao, G., Pandurangan, K., Sultana, F., (2007) “Studies on the Pull-out Strength of Ribbed Bars in High-strength Concrete”,

(10) Ross, A.D., (1958) “Creep of Concrete under Variable Stress”, Journal of the American Concrete Institute, March 1958, pp 747.

(11) Rusch, Hubert (1960), “Researches Toward a General Flexural Theory for Structural Concrete”, ACI Journal, July 1960, pp 1-25.

(12) Tasevski, Darko (2019), “Time-dependent strength of concrete in compression and shear”, École Polytechnique, June 2019, pp 12-19.

(13) Walker, P. R., Batayneh, M. K., Regan, P. E. (1997). “Bond Strength Test on Deformed Reinforcement in Normal Weight Concrete”, *Materials and Structures* Vol. 30, August-September 1997, pp 424-429.

(14) Wardhana, K. and Hadipriono, F. (2003). “Study of Recent Building Failures in the United States,” Journal of Performance of Constructed Facilities, pp 151-158.

(15) Wight, James K., MacGregor, James G., (2009) “Reinforced Concrete Mechanism & Design”, 6E.

APPENDIX

Creep Deflection Calculation

$$\rho' = \frac{A_s'}{bd} = \frac{0.22\ in^2}{(5.5\ in)(0.8125\ in)} = 0.0492$$

Find λ_Δ, the multiplier which determines expected creep deflection:

$$\lambda_\Delta = \frac{\xi}{1 + 50\rho'} = \frac{0.6}{1 + (50 * 0.0492)} = 0.1733$$

ξ = 0.6 at 28 days

$$\lambda_\Delta = \frac{0.65}{1 + (50 * 0.0492)} = 0.1878$$

ξ = 0.65 at 40 days

Total deflection from creep

$$\Delta_{creep} = \Delta_i \lambda_\Delta$$

B-SL-81

$$\Delta_{creep} = 0.218" * 0.1733 = 0.0378"$$

B-SL-86

$$\Delta_{creep} = 0.423" * 0.1878 = 0.0794"$$

B-SL-92

$$\Delta_{creep} = 0.492" * 0.1733 = 0.0749"$$